Heliyon 10 (2024) e35645

Contents lists available at ScienceDirect

Heliyon

journal homepage: www.cell.com/heliyon

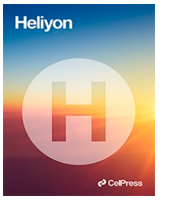

Research article

In vivo identification of bioactive components of *Poria cocos* for adjusting mitochondria against metabolic dysfunction-associated fatty liver disease

Yanjuan Li [a,b,1], Pengquan Wang [a,b,1], Huan Yang [a,b,1], Jinbiao He [a,b], Yu Yang [a,b], Yuxuan Tao [a,b], Min Zhang [a,b], Mei Zhang [a,b], Jie Yu [a,b,**], Xingxin Yang [a,b,*]

[a] College of Pharmaceutical Science, Yunnan University of Chinese Medicine, 1076 Yuhua Road, Kunming, 650500, China
[b] Yunnan Key Laboratory of Southern Medicine Utilization, 1076 Yuhua Road, Kunming, 650500, China

ARTICLE INFO

Keywords:
Fatty liver
Mitochondria
Pharmacodynamic ingredients
Poria cocos

ABSTRACT

Currently, no specific treatment exists to alleviate metabolic dysfunction-associated fatty liver (MAFLD). Previously, *Poria cocos* (PC) effectively relieved MAFLD, but its bioactive components are still unknown. The bioactive substances in PC that regulate mitochondria function to alleviate MAFLD were thus determined. The L02 hepatocyte model induced by fat emulsion and the MAFLD rat model induced by a high-fat diet (HFD) were developed to explore the efficacy of PC against MAFLD. The activity of PC-derived components in the liver mitochondria of HFD-fed rats was evaluated using the L02 hepatocyte model. Additionally, the PC-derived components from the liver mitochondria were identified by ultra-high performance liquid chromatography/mass spectrometry. Finally, the *anti*-steatosis ability of PC-derived monomers and monomers groups was evaluated using the adipocyte model. PC maintained the mitochondrial ultrastructure, alleviated mitochondrial oxidative stress, and regulated the energy metabolism and the fatty acid β oxidation to relieve lipid emulsion-induced cellular steatosis and HFD-induced MAFLD. PC-derived components entering the liver mitochondria inhibited oxidative stress injury and improved the energy metabolism to fight cellular steatosis. Additionally, 15 chemicals were identified in the PC-treated rat liver mitochondria. These identified chemical molecules and molecule groups in the mitochondria prevented cellular steatosis by regulating mitochondrial

Abbreviations: ACADL, long chain Acyl-coenzyme A dehydrogenase; ALT, alanine transaminase; AST, aspartate transaminase; ATPase, ATP synthase; BCA, bicinchoninic acid; Complex-I/II, mitochondrial respiratory chain complex I and II; CPT-1 B, carnitine palmitoyl transferase-1 B; DEA, dehydroeburicoic acid; DMA, dehydrotrametenolic acid; DMSO, Dimethyl sulfoxide; DPA, dehydropachymic acid; DTA, dehydrotumulosic acid; ECHS, short chain Enoyl-coenzyme A hydratase; FAS, fatty acid synthetase; FC, fenofibrate control group; GSH, glutathione; HDL-C, high density lipoprotein cholesterol; HE, hematoxylin and eosin; HFD, high-fat diet; HPC, high-dose PC extract group; HTA, 16α-hydroxytrametenolic acid; LDL-C, low density lipoprotein cholesterol; LPC, low-dose PC extract group; MAFLD, metabolic dysfunction associated fatty liver; MDA, malondialdehyde; MME, liver mitochondrial extracts from model group; MOD, model group; MS, mass spectrometry; NC, normal control group; PAB, poricoic acid B; PAG, poricoic acid G; PBS, phosphate buffered saline; PC, *Poria cocos*; PCME, liver mitochondrial extracts from high-dose of PC extract group; PCMM, PC-derived monomers group in mitochondria; PPAC, polyporenic acid C; PPAR-α, peroxide proliferator activated receptor α; qRT-PCR, quantitative real-time PCR; ROS, reactive oxygen species; SD, standard deviation; SOD, superoxide dismutase; TC, total cholesterol; TCMs, traditional Chinese medicines; TG, triglycerides; UCP-2, uncoupling protein 2; UHPLC, ultra-high performance liquid chromatography.

* Corresponding author. College of Pharmaceutical Science, Yunnan University of Chinese Medicine, 1076 Yuhua Road, Kunming, 650500, China
** Corresponding author. College of Pharmaceutical Science, Yunnan University of Chinese Medicine, 1076 Yuhua Road, Kunming, 650500, China
E-mail addresses: cz.yujie@gmail.com (J. Yu), yxx78945@163.com (X. Yang).
[1] These authors contributed equally to this work.

https://doi.org/10.1016/j.heliyon.2024.e35645
Received 7 March 2024; Received in revised form 25 June 2024; Accepted 1 August 2024
Available online 3 August 2024

oxidative stress and energy metabolism. PC restores mitochondrial structure and function, alleviating MAFLD, which is related to oxidative stress, energy metabolism, and fatty acid β oxidation. The identified 15 components may be the main effective PC components regulating mitochondria function to alleviate MAFLD. Thus, PC may be a promising mitochondrial regulator to prevent MAFLD.

1. Introduction

Metabolic dysfunction associated fatty liver (MAFLD) is the most common chronic liver disease, closely related to metabolic disorders, including centripetal obesity, dyslipidemia, hypertension, hyperglycemia, and abnormal, persistent liver dysfunction [1]. Its pathological process temporarily follows the "three strikes" process consisting of steatosis, lipotoxicity, and inflammation. However, although MAFLD poses major clinical and public health burdens worldwide, it lacks a definitive treatment strategy. At present, MAFLD is mainly managed by promoting weight loss by changing lifestyle, diet control, physical activity, and controlling its major risk factors. Therefore, there is an urgent need to find new drugs for treating MAFLD [2–4].

Mitochondria are organelles maintaining growth and function in eukaryotic cells. They are involved in oxidative phosphorylation, energy generation, metabolic homeostasis, redox regulation, and apoptosis [5]. In liver tissues, MAFLD is characterized by changes in mitochondrial ultrastructure and dynamics, decreased respiratory chain complex activity, and impaired ATP synthesis ability. MAFLD also induces increased fat production and decreased fatty acid β oxidation, resulting in the accumulation of triglycerides in hepatocytes [6]. Subsequently, excessive lipid accumulation promotes intracellular oxidative stress response and reactive oxygen species (ROS) production, leading to mitochondrial dysfunction and cell toxicity, exacerbating MAFLD development [7]. However, traditional Chinese medicines (TCMs), such as *Polygonatum kingianum* [8] and *Cinnamomum cassia* [9], regulate mitochondrial function alleviating MAFLD.

Moreover, *Poria cocos* (PC), a fungus used as medicine and food, alleviates liver steatosis by regulating lipid metabolism, inhibiting endoplasmic reticulum stress, and activating AMPK-dependent autophagy [10]. PC has been used as a TCM in China for over two thousand years. Its chemical constituents mainly include triterpenes, polysaccharides, proteins, and amino acids, characterized by anti-inflammatory activity, immunomodulatory properties, anticancer properties, anti-hyperglycemia effects, and blood lipid regulation ability [11,12]. PC also has potential *anti*-MAFLD effects [12]. However, the active ingredients of PC against MAFLD remain unclear. Besides, it is unknown whether PC alleviates MAFLD by regulating mitochondrial function.

A previous research developed an efficient mitochondrial pharmacology and pharmacochemistry strategy for searching bioactive substances in TCMs (*Polygonum multiflorum* and *Polygonum cuspidatum*) that regulate mitochondria function to relieve MAFLD [13]. The results demonstrated that this strategy effectively identifies mitochondria-adjusted ingredients in TCMs *in vivo*.

Thus, in the present study, mitochondrial pharmacology and pharmacochemistry determined the potential of mitochondria-targeted bioactive components in PC extract to alleviate MAFLD triggered by a high-fat diet (HFD). Additionally, the efficacy and potential mechanisms of PC against MAFLD were evaluated using *in vitro* and *in vivo* pharmacological experiments. The results revealed that PC restored mitochondrial structure and function to alleviate MAFLD, which may be related to oxidative stress and energy metabolism. Besides, 15 potentially effective PC components were identified in regulating mitochondria to prevent MAFLD.

2. Methods and materials

2.1. Reagents, chemicals and materials

Human hepatocyte cell line L02 (iCell-h054) was sourced from Cellverse Bioscience Technology Co., Ltd. (Shanghai, China). RPMI-1640 culture medium was purchased from XP Biomed Ltd. (Shanghai, China). Fetal bovine serum was purchased from Procell Life Science & Technology Co., Ltd. (Wuhan, China). Penicillin-streptomycin, trypsin solution, and phosphate-buffered saline (PBS) were provided by Saiguo Technology Co., Ltd. (Guangzhou, China). Basic feed and a high-fat diet containing 1 % cholesterol, 10 % refined lard, 10 % egg yolk, and 79 % basic feed were provided by Beijing Keaoxieli Feed Co., Ltd. (Beijing, China). Standards including dehydrotrametenolic acid (DMA, ≥98 % purity), dehydrotumulosic acid (DTA, ≥98 % purity), dehydropachymic acid (DPA, ≥99 % purity), dehydroburicoic acid (DEA, ≥99 % purity), polyporenic acid C (PPAC, ≥99 % purity), and 16α-hydroxytrametenolic acid (HTA, ≥97 % purity) were purchased from Chengdu Pufeide Biotech Co., Ltd. (Chengdu, China). Poricoic acid B (PAB, ≥98 % purity) and poricoic acid G (PAG, ≥98 % purity) were sourced from Jiangsu Aikang Biomedical Research and Development Co. Ltd. (Jiangsu, China) and Wuhan ChemFaces Biochemical Co., Ltd. (Wuhan, China), respectively. Kits for determining triglycerides (TG), total cholesterol (TC), alanine transaminase (ALT), aspartate transaminase (AST), low-density lipoprotein cholesterol (LDL-C), high-density lipoprotein cholesterol (HDL-C), malondialdehyde (MDA), superoxide dismutase (SOD), glutathione (GSH), ATP synthase (ATPase) levels, and assay kits for the determination of proteins (bicinchoninic acid [BCA] kit) were purchased from Nanjing Jiancheng Bioengineering Institute (Nanjing, China). Respiratory chain complex I and II (Complex-I/II) detection kits were purchased from Jiangsu Enzyme Immune Industrial Co., Ltd. (Jiangsu, China). HPLC-grade methanol and acetonitrile were purchased from Sigma Aldrich Trade Co., Ltd. (Shanghai, China). Primers were designed and synthesized by Generay Biotech Co., Ltd. (Shanghai, China). M-MLV Reverse Transcriptase, RNA-easy Isolation Reagent, and ChamQ Universal SYBR qPCR Master Mix were purchased from Vazyme Biotech Co., Ltd. (Nanjing, China). Dimethyl sulfoxide (DMSO), TriQuick reagent for extracting total RNA, and Highly Efficient RIPA

Table 1
The primers sequences for qRT-PCR assay used in PC-treated L02 cells.

Gene	NCBI reference sequence accession number	Sequence (5′–3′)	Temperature (°C)
CPT-1B	NM_001031847.3	Forward: TGGTGCTCAAGTCATGGTGG	56.63
		Reverse: TGCCTGCACGTCTGTATTCT	56.43
FAS	NM_000043.6	Forward: GCATCTGGACCCTCCTACCT	55.9
		Reverse: CTGGAGGACAGGGCTTATGG	55.11
UCP-2	NM_001381943.1	Forward: TCGGAGATACCAAAGCACCG	55.49
		Reverse: TTGGCTTTCAGGAGGGCATC	55.89
GAPDH	NM_001256799.3	Forward: CTGGGCTACACTGAGCACC	55.46
		Reverse: AAGTGGTCGTTGAGGGCAATG	57.03

Tissue/Cell Lysate were provided by Solarbio Science & Technology Co., Ltd. (Beijing, China). Deionized water was purified by a Milli-Q Water Purification System Purification System (Millipore, Billerica, MA, USA). All other reagents used were of analytical reagent grade or higher. The dried PC samples were collected from Jinggu County (Pu'er, China) and stored at the Key Laboratory of Southern Medicine Utilization, Yunnan University of Chinese Medicine (Kunming, China).

2.2. Preparation of PC extract

Dried PC samples were pulverized and extracted with a three-fold volume of 75 % ethanol at 60 °C for 2 h. The filtrate was collected after leaching. The residue was extracted sequentially with a three-fold volume of 75 % ethanol at 60 °C for 2 h, and the extracted liquid was filtered. Next, the two filtrates were condensed using an N-1100D-WD rotatory evaporator (Shanghai Ailang Instrument Co., LTD, Shanghai, China), and the concentrate was dried on an FD 5-3 freeze-dryer (SIM International Group Co., Ltd., Newark, DE, USA). The obtained dried PC extracts with a yield of 2.66 % were then stored in a desiccator, awaiting further analysis.

Subsequently, the chemical composition of the PC extract was determined as previously described [14]. Briefly, the PC extract was loaded into the Waters 2695 Series HPLC system fitted with a Symmetry Shield RP-C18 (4.6 mm × 250 mm, 5um) column and UV–vis detector. The analytical conditions were as follows: (1) the injection volume, column temperature, flow rate, and detection wavelength were set at 20 μL, 30 °C, 1.0 mL/min, and 243 nm, respectively; (2) the mobile phase comprised of acetonitrile (A) and 0.1 % aqueous phosphoric acid solution (B). The elution gradient was as follows: 0–50 min, 44%A; 50–53 min, 44%A-58%A; 53–60 min, 58%A; 60–70 min, 58%A-75%A; 70–88 min, 75%A; 88–95 min, 75%A-81%A; 95–100 min, 81%A; 100–110 min, 81%A. PAB, PPAC, DTA, DPA, and DEA, used as references, were precisely weighed and dissolved in methanol to 0.18, 0.62, 0.63, 0.64, and 0.51 mg/mL. At the same time, about 51.55 mg PC extract was accurately weighed and dissolved in 5 mL of methanol. PAB, PPAC, DTA, DPA, and DEA peaks were distinguished by comparing their retention times with those of standards. The PAB, PPAC, DTA, DPA, and DEA contents in the PC extract were 0.35, 1.09, 0.94, 0.68, and 0.01 %, respectively.

2.3. PC extract anti-steatosis ability in vitro

The L02 cells were cultured in RPMI 1640 medium supplemented with 10 % fetal bovine serum and 1 % penicillin-streptomycin and incubated at 37 °C, 5 % carbon dioxide, and 95 % humidity. Next, the cells were seeded in 96-well plates at a density of 100,000 cells per well for 24 h. Subsequently, the cells were cultured in RPMI 1640 medium containing 0.2 % serum for 12 h and in RPMI 1640 medium containing 5 % fat emulsion for 24 h. The cells were then treated with PC extract (0.05, 0.1, 0.2, or 0.4 mg/mL), fenofibrate (FC, 150 μM), or RPMI 1640 medium (normal control). After 24 h, the cells were harvested.

Subsequently, the protein concentration in the harvested cells was determined by the BCA method. In addition, the ALT, AST, ATPase, Complex-I/II, GSH, SOD, TC, and TG levels were determined using the commercial kits according to the manufacturer's instructions on a Spectra Max Plus 384 microplate reader (Molecular Devices, Sunnyvale, CA, USA). The cells were then washed twice in ice-cold PBS and fixed with 2.5 % paraformaldehyde for 30 min. Next, the cells were treated with 60 % isopropanol and cultured for 5 min before being stained with 0.2 % oil red O solution for 30 min. After staining, the cells were washed in two changes of PBS and stained with hematoxylin for 3 min. Images of the stained cells were captured by the CX31 Olympus imaging system (Olympus Corporation, Tokyo, Japan). Quantification of oil red O positive staining areas was measured by software ImageJ (NIH, USA).

In addition, the L02 cell mitochondrial ultrastructure was observed under a transmission electron microscope (Hitachi HT 7700, Hitachi Ltd, Tokyo, Japan). Briefly, the glass slides were immersed in RPMI 1640 medium containing L02 cells. The cell-filled slides were sequentially fixed in 1 % osmic acid at 20 °C for 2 h, washed with PBS three times for 15 min each time, and dehydrated through a 50, 70, 80, 90, 95, and 100 % ethanol gradient, and 100 % acetone for 15 min each time. Subsequently, the cells were infiltrated overnight (2:1 acetone: embedding medium) before they were sliced into ultra-thin slices (60–80 nm) using an ultra-thin microtome (Leica RM 2135, Leica Ltd., Hesse, Germany). The obtained slices were stained with 2 % uranium acetate saturated alcohol solution and lead citrate for 15 min each and dried overnight at room temperature. Finally, the cell slides were observed under a transmission electron microscope.

Fatty acid β oxidation genes in L02 cells were also assayed. The total RNA was extracted from the treated cells with the RNA-easy Isolation Reagent following the manufacturer's instructions. The extracted RNA was reverse transcribed using M-MLV Reverse Transcriptase at 25 °C for 5 min, 42 °C for 3 min, and 85 °C for 5 s to synthesize the cDNA. Finally, the gene expression levels were quantified by quantitative real-time PCR (qRT-PCR) using the SYBR qPCR Master Mix reagent following the manufacturer's

Table 2
The primers sequences for qRT-PCR assay used in livers of PC-treated MAFLD rats.

Gene	NCBI reference sequence accession number	Sequence (5′–3′)	Temperature (°C)
ACADL	NM_012819.3	Forward: CATACCCGTCCGTGCTCAA	59.84
		Reverse: CCTGCCAAGTGGTCTCCTCC	60.11
ECHS	NM_078623.2	Forward: CGAGCAGTCGGCAAATCA	58.47
		Reverse: CAGTGGCAAAGGTGGAATAGAA	59.61
PPAR-α	NM_013196.2	Forward: GAGGTCCGCATCTTTCACT	54.54
		Reverse: ACGGTTTCCTTAGGCTTTT	53.77
GAPDH	NM_017008.4	Forward: AGTTGCGTTACACCCTTTCTTG	59.03
		Reverse: TCACCTTCACCGTTCCAGTTT	59.44

instructions. The gene expression levels were normalized to the internal control (GAPDH) and computed using the $2^{-\Delta\Delta CT}$ method. The primers used in the qRT-PCR reactions are listed in Table 1.

2.4. Evaluation of the PC extract anti-MAFLD ability in vivo

2.4.1. Animals and experimental design

Healthy male Sprague Dawley rats (200 ± 20 g) were obtained from Dashuo Biotech. Co., Ltd. (Hunan, China). The rats were acclimatized in a specific pathogen-free environment (24.2 °C, 45 % ± 10 % humidity and 12 h light/dark cycle) with free access to food and water for one week and then randomly assigned into five groups (n = 6 per group): the normal control group (NC, normal saline), model group (MOD, normal saline), fenofibrate group (FC, 20 mg/kg/d), low-dose PC extract group (LPC, 56 mg/kg/d), and high-dose PC extract group (HPC, 169 mg/kg/d). The low-dose PC extract used in rat experiments was calculated according to the known PC dose of humans (10 g/day/person), which was recorded in the Chinese Pharmacopoeia (2020). All treatments were intragastrically administered once daily for 12 consecutive weeks. In addition, rats in all groups, except the NC group, were fed on a HFD for 12 weeks to trigger MAFLD. The feed intake of all rats was recorded daily, and body weights were determined once a week. All the animal experiment protocols were reviewed and approved by the Institutional Ethical Committee on Animal Care and Experimentations of the Yunnan University of Chinese Medicine (Kunming, China) according to the Guide for the Care and Use of Laboratory Animals published by the National Institutes of Health.

2.4.2. Sample collection

At the end of the 12 weeks, the rats were administered the corresponding test samples. After 1 h, the rats were anesthetized with 10 % pentobarbital sodium. Blood was taken from the abdominal aorta and allowed to clot at 4 °C. Next, the blood samples were centrifuged (3500×g/15 min/4 °C) and stored at −80 °C, awaiting further analysis. In addition, the rat organs, including the liver, kidney, and spleen, were immediately removed, weighed, and stored at −80 °C. Before storage, some liver samples were isolated for oil red O staining and hematoxylin-eosin (HE) staining.

2.4.3. Oil red O and HE staining

Liver samples were fixed in 4 % paraformaldehyde, embedded in paraffin, sectioned at 5 μm, and stained with HE. The liver samples were fixed, embedded in cryo-embedding compound for oil red O staining, and frozen at −20 °C for 30 min. Frozen liver samples were sectioned into 8 μm and stained with oil-red O dye. Finally, the stained sections were visualized under a CX31 Olympus imaging system (Olympus Corporation, Tokyo, Japan). Quantification of oil red O positive staining areas was measured by software ImageJ (NIH, USA).

2.4.4. Determination of serum and liver bio-parameters

The ALT, AST, HDL-C, LDL-C, TC, and TG levels in the serum samples were determined using a biochemical analyzer (Beckman CX4, Roche, Germany). Briefly, 0.1 g of the liver was weighed, and a liver homogenate was prepared with a 9-fold volume of physiological saline. The homogenate was centrifuged at 2000 rpm/min for 10 min. Finally, the TC, TG, LDL-C, HDL-C, ALT, and AST levels in the supernatant were determined using the commercial kits according to the manufacturer's instructions.

2.4.5. Evaluation of liver mitochondrial indexes

Mitochondria were isolated from the rat liver per the mitochondrial isolation protocol and resuspended in normal saline [15]**.** Next, the protein concentration in the mitochondrial suspension was determined using the BCA method. In addition, the MDA, SOD, GSH, ATPase, and Complex-I/II levels in the mitochondrial suspension were determined using the commercial kits according to the manufacturer's instructions.

2.4.6. Determination of fatty acid β oxidation related genes in the liver

Briefly, 0.1 g of the rat liver tissues were weighed and ground in liquid nitrogen. The tissues were then rapidly homogenized in RNA-easy Isolation Reagent to extract the total RNAs according to the manufacturer's protocol. Subsequently, the extracted total RNA was reverse transcribed into cDNA using M-MLV Reverse Transcriptase. Finally, the expression level of fatty acid β oxidation-related genes was quantified by qRT-PCR using the SYBR qPCR Master Mix reagent. The primers used in the qRT-PCR reactions are listed in

Table 3
The primers sequences for qRT-PCR assay used in PCMM-treated L02 cells.

Gene	NCBI reference sequence accession number	Sequence (5′–3′)	Temperature (°C)
ACADL	NM_001608.4	Forward: AGCCACCAAGATGCTGACAT	55.22
		Reverse: GGCCTGCACTTCCATAGAGTT	55.9
ECHS	NM_004092.4	Forward: GCCTCGGGTGCTAACTTTGA	55.96
		Reverse: GCCATCGCAAAGTGCATTGA	55.82
PPAR-α	NM_001113418.1	Forward: GAAAGGCCAGTAACAATCCACC	55.63
		Reverse: CGCCTCCTTGTTCTGGATGC	57.06
GAPDH	NM_001256799.3	Forward: CTGGGCTACACTGAGCACC	55.46
		Reverse: AAGTGGTCGTTGAGGGCAATG	57.03

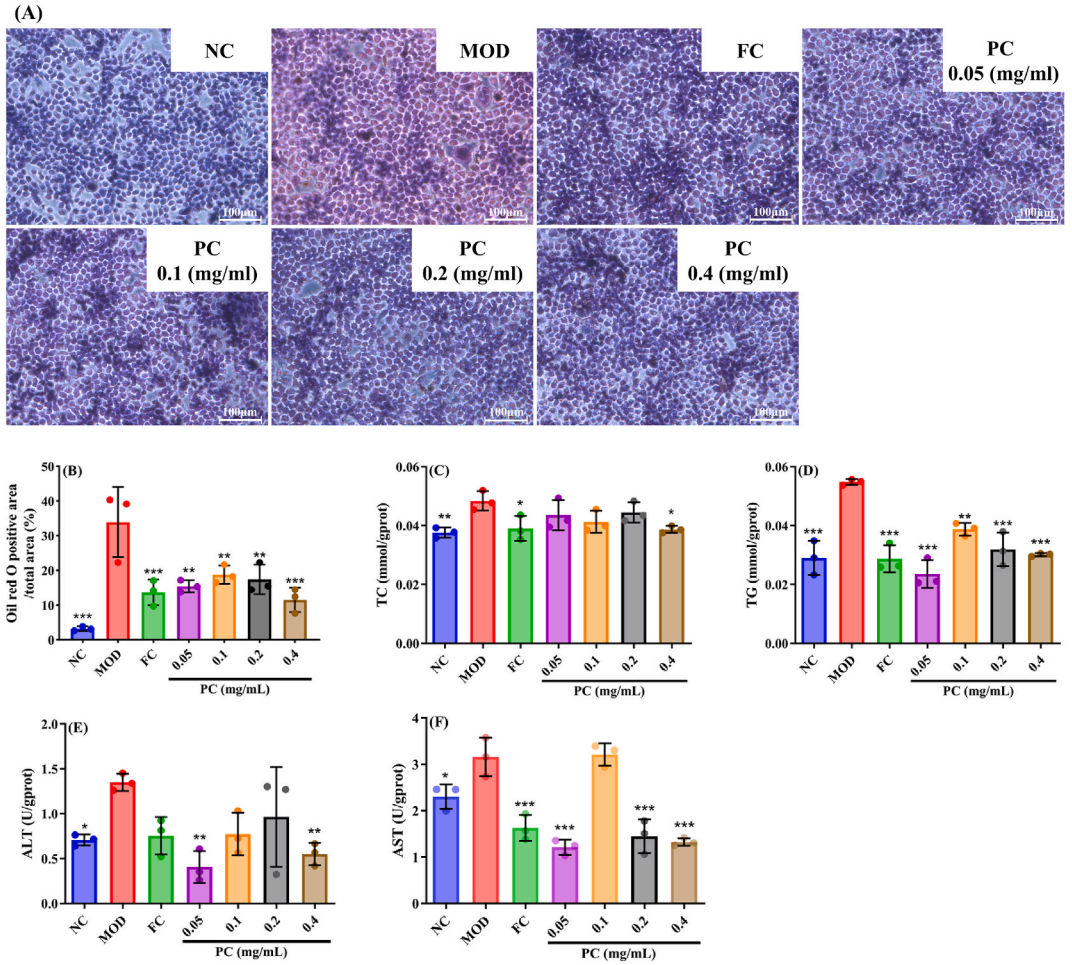

Fig. 1. Effects of PC extract on fat emulsion-induced L02 adipocytes. Fat accumulation in oil-red O-stained cells (A). Quantitative analysis of oil red O positive area in cells (B). (C) TC; (D) TG; (E) ALT; and (F) AST levels in the fat emulsion-induced L02 adipocytes. Data were obtained from 3 independent measurements. $^{*}P < 0.05$, $^{**}P < 0.01$, $^{***}P < 0.001$ vs. MOD group. ALT, alanine transaminase; AST, aspartate transaminase; FC, fenofibrate control group; MOD, model group; NC, normal control group; PC, *Poria cocos*; TC, total cholesterol; TG, triglyceride.

Table 2.

2.5. Activity assay and structural assignment of PC-derived ingredients in HFD-fed rat liver mitochondria

2.5.1. Preparation of liver mitochondrial extracts

Rat liver mitochondria from MOD and HPC groups were isolated following the previously described method [15]. The obtained mitochondria were sequentially suspended in 80 % methanol, ultrasonicated for 20 min, and centrifuged at 1000 g for 25 min. The supernatant was collected and dried under mild nitrogen purge to obtain mitochondrial extracts.

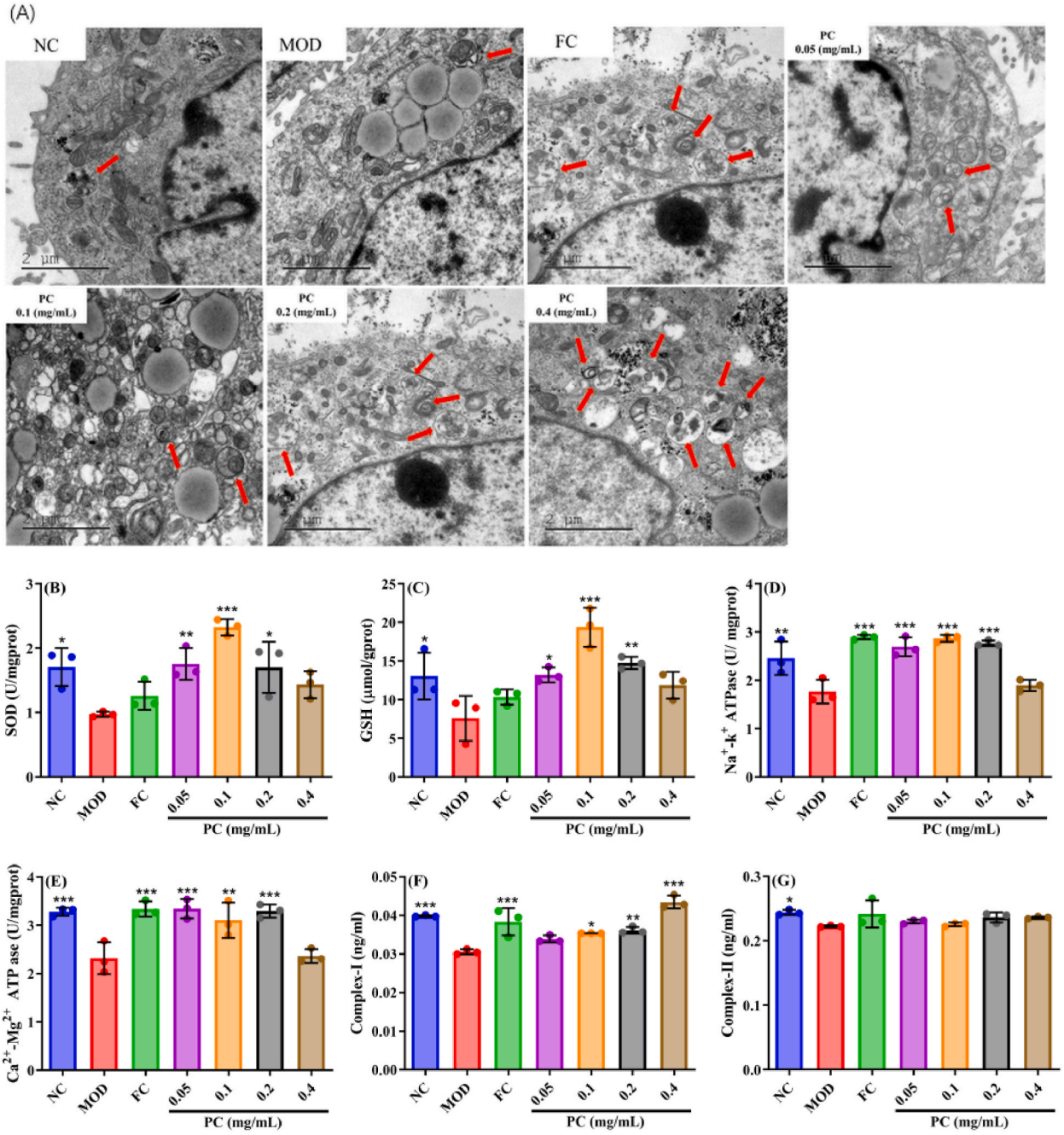

Fig. 2. Effect of PC extract on L02 adipocytes mitochondrial state. L02 cells mitochondrial ultrastructures (A). (B) SOD; (C) GSH (D) Na^{+}-K^{+}-ATPase, (E) Ca^{2+}-Mg^{2+}-ATPase, (F) Complex-I and (G) Complex-II levels in the L02 cell mitochondria. Data represent the average of three independent measurements. $^{*}P < 0.05$, $^{**}P < 0.01$, $^{***}P < 0.001$ vs. MOD group. ATPase, ATP synthase; Complex-I/II, mitochondrial respiratory chain complex I and II; FC, fenofibrate control group; GSH, glutathione; MOD, model group; NC, normal control group; PC, *Poria cocos*; SOD, superoxide dismutase.

2.5.2. In vitro determination of the anti-steatosis ability of PC-derived components in mitochondria (mitochondrial pharmacology)

First, the L02 cells were induced by fat emulsion. Next, the cells were treated with FC (150 μM) and liver mitochondrial extracts (50, 100, or 200 μg/mL) from MOD group (MME) and HPC group (PCME) for 24 h. The protein concentration in the cell lysates was determined by the BCA method. At the same time, the TG, TC, AST, GSH, SOD, and Complex-I/II levels in the cells were determined using commercially available diagnostic kits following the manufacturer's instructions. In addition, the cells were stained with Oil Red O and visualized as described in section 2.3.

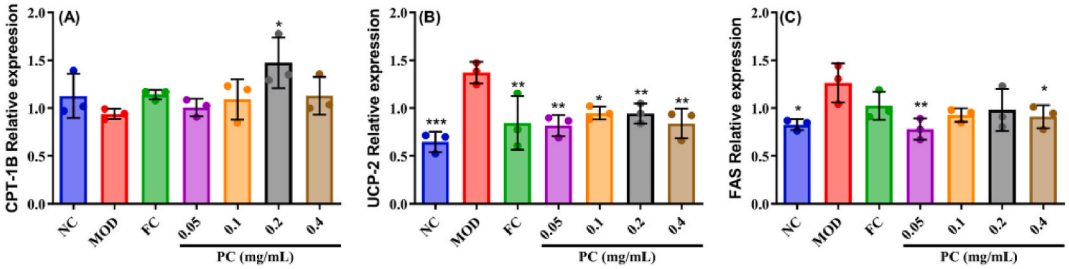

Fig. 3. Effects of PC extract on the mRNA expression levels of fatty acid β oxidation related genes of L02 adipocytes. The mRNA expression levels of (A) CPT-1B, (B) UCP-2, and (C) FAS. Data represent the average of three independent measurements. *$P < 0.05$, **$P < 0.01$, ***$P < 0.001$ vs. MOD group. CPT-1 B, carnitine palmitoyltransferase 1 B; FAS, fatty acid synthase; FC, fenofibrate control group; MOD, model group; NC, normal control group; PC, *Poria cocos*; qRT-PCR, quantitative real-time PCR; UCP-2, uncoupling protein 2.

2.5.3. Structural assignment of PC-derived ingredients in mitochondria (mitochondrial pharmacochemistry)

PC extracts and liver mitochondrial extracts isolated from the MOD and HPC groups were redissolved in methanol and filtered through a 0.22 μm Millipore filter (Bedford, MA, United States). The filtrate was analyzed by an ultra-high performance liquid chromatography (UHPLC) Dionex Ultimate 3000 system coupled with a Thermo Scientific Q-Exactive TM hybrid quadrupole-orbitrap mass spectrometry (MS) (Thermo Fisher Scientific, San Jose, CA, United States) as described previously [13].

2.5.4. Determination of anti-steatosis capability of PC-derived monomers and monomers group in mitochondria in vitro

Fat emulsion-induced steatosis L02 cells were stimulated with FC (150 μM), 10, 20, and 40 μM of PC-derived monomers (DMA, DTA, DPA, DEA, PPAC, HTA, and PAG), and 5, 10, or 20 μg/mL of monomers group (consisting of HTA, PAG, DMA, DTA, DPA, DEA and PPAC in the ratio 15.12: 20.75: 7.57: 1: 21.84: 31.77: 4.38; their concentration ratio in the PCME extract, based on the chromatographic peak obtained in the PCME UHPLC/MS assay). Based on the earlier investigations conducted by our team, the monomer and monomers group dosage spectrum sourced from traditional Chinese medicines have been established to fall within the range of 1–100 μM and 1–100 μg/mL, respectively. It has been indicated that heightened efficacy is correlated with increasing dosage levels [12,13]. The dosages for monomer and monomers group used in the present study were thus set at these regimens. The protein concentration in the cell lysates was determined by BCA assay. In addition, the TG, TC, SOD, GSH, Complex-I/II, and ATPase levels in the cells were determined using diagnostic kits following the manufacturer's instructions. Additionally, fatty acid β oxidation-related gene expression in the monomer group-treated cells was detected by qRT-PCR according to the method described in section 2.3. The primers used in the qRT-PCR reactions are listed in Table 3.

2.6. Statistical analysis

All values are presented as the mean ± standard deviation (SD). All statistical analyses were performed using GraphPad Prism version 5.01 software for Windows (San Diego, California, USA). Comparisons between groups were performed using one-way ANOVA and single comparisons using unpaired Student's t-test at *$P < 0.05$, **$P < 0.01$, or ***$P < 0.001$ significance levels.

3. Results

3.1. Effects of PC extract on fat emulsion-induced adipocytes

The fat emulsion stimulation increased the intracellular lipid level (Fig. 1A and B). In addition, it significantly increased the TC, TG, ALT, and AST levels ($P < 0.05$, $P < 0.01$, $P < 0.001$) after 24 h of fat emulsion stimulation (Fig. 1C–F). However, treatment with PC extract significantly prevented the accumulation of lipids in the cells. Additionally, it significantly decreased the TC, TG, ALT, and AST levels ($P < 0.05$, $P < 0.01$, $P < 0.001$), suggesting that PC extract inhibited fat emulsion-induced steatosis in L02 cells.

After the cells were treated with fat emulsion, the inner and outer membranes and cristae of mitochondria were blurred with the unclear matrix and a few autophagosomes (shown by the red arrow) (Fig. 2A). However, treatment with PC extract significantly improved the mitochondrial ultrastructure and the number of autophagosomes. Furthermore, fat emulsion stimulation for 24 h significantly decreased the GSH, SOD, Na^+-K^+-ATPase, Ca^{2+}-Mg^{2+}-ATPase, and Complex-I levels ($P < 0.05$, $P < 0.01$, $P < 0.001$) (Fig. 2B–F), but was significantly increased ($P < 0.05$, $P < 0.01$, $P < 0.001$) after treatment with PC extract. Additionally, fat emulsion stimulation for 24 h significantly decreased the Complex-II level ($P < 0.001$), but was not noticeably affected by PC treatment (Fig. 2G). These findings suggest that PC extract prevented the damage to mitochondrial structure and function and enhanced the mitochondrial autophagy, alleviating the L02 cells steatosis.

Cellular treatment with fat emulsion significantly increased the mRNA expression level of uncoupling protein 2 (UCP-2) and fatty acid synthetase (FAS) ($P < 0.05$, $P < 0.001$), with a downward trend in the mRNA expression levels of carnitine palmitoyl transferase-1 B (CPT-1B) (Fig. 3). Interestingly, PC extract treatment significantly reduced the mRNA expression levels of UCP-2 and FAS and significantly increased the mRNA expression level of CPT-1 B. These results indicate that the PC extract promoted fatty acid β oxidation

Table 4
Effects of PC extract on body weight, food intake, and organ indices of rats.

	NC	MOD	FC	LPC	HPC
Initial body weight (g)	228.33 ± 8.41	227.71 ± 16.21	235.33 ± 14.92	224.14 ± 10.71	225.14 ± 7.24
Final body weight (g)	562.50 ± 35.32	616.33 ± 38.22	587.33 ± 36.06	609.17 ± 58.01	590.00 ± 22.35
Body weight gain (g)	334.17 ± 26.92	388.62 ± 22.00	352.00 ± 21.14	385.02 ± 47.33	364.86 ± 15.11
Food intake (g)	16044	12586	12485	13050	12674
Liver index (%)	2.19 ± 0.24***	3.26 ± 0.11	3.85 ± 0.04***	2.81 ± 0.09***	2.88 ± 0.12***
Kidney index (%)	0.56 ± 0.02	0.55 ± 0.03	0.55 ± 0.03	0.51 ± 0.02	0.51 ± 0.02
Spleen index (%)	0.15 ± 0.01	0.16 ± 0.01	0.15 ± 0.03	0.15 ± 0.01	0.15 ± 0.01

***$P < 0.001$ vs. MOD group. Values represent the mean ± SD from six animals. FC, fenofibrate control group; HPC, high-dose PC extract group; LPC, low-dose PC extract group; MOD, model group; NC, normal control group.

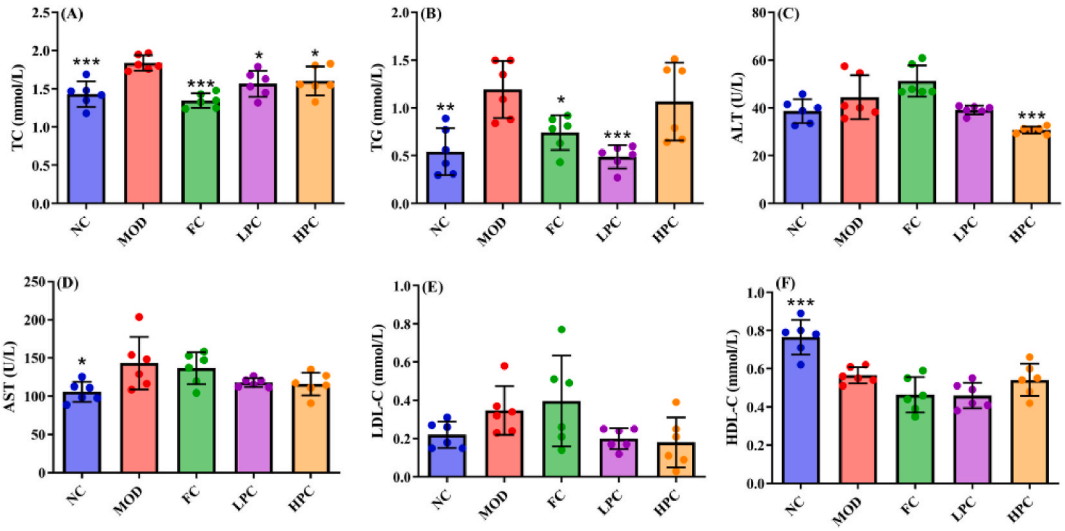

Fig. 4. Effects of PC extract on serum lipid contents of HFD-fed rats. The (A) TC, (B) TG, (C) ALT, (D) AST, (E) LDL-C, and (F) HDL-C levels in the serum. *$P < 0.05$, **$P < 0.01$, ***$P < 0.001$ vs. MOD group. ALT, alanine transaminase; AST, aspartate transaminase; FC, fenofibrate control group; HDL-C, high density lipoprotein cholesterol; HFD, high-fat diet; HPC, high dose of *poria cocos* extract; LDL-C, low density lipoprotein cholesterol; LPC, low dose of *poria cocos* extract; MOD, model group; NC, normal control group; TC, total cholesterol; TG, triglyceride.

to reduce fat emulsion-induced steatosis in L02 cells.

3.2. Effects of PC extract on HFD-fed rats

3.2.1. Effects of PC extract on body weight, food intake, and organ indexes

As shown in Table 4, after 12 weeks of HFD feeding, the liver index increased significantly ($P < 0.001$), the body weight and spleen index showed an upward trend, and the kidney index was not affected. However, after treatment with PC extract, the liver index significantly reduced ($P < 0.001$), with a downward trend in the body weight and spleen and kidney indexes. Besides, there were no significant differences in food intake between the groups during the feeding period. These indicate that weight gain and hepatomegaly were alleviated by PC extract.

3.2.2. Effects of PC extract on serum and liver lipid contents

After 12 weeks of HFD-feeding, the TC, TG, and AST levels were significantly increased ($P < 0.05$, $P < 0.01$, $P < 0.001$), while the HDL-C levels were significantly decreased ($P < 0.001$). At the same time, the ALT, and LDL-C levels showed an upward trend (Fig. 4). However, after treatment with PC extract, the TC, TG, and ALT levels were significantly decreased ($P < 0.05$, $P < 0.001$), and the AST and LDL-C levels showed a downward trend, implying that the PC extract relieved HFD-induced dyslipidemia.

Moreover, the oil red O staining on the liver revealed severe lipid accumulation and hepatocyte degeneration in the rat liver after 12 weeks of HFD feeding (Fig. 5A and C). However, the number of lipid droplets in the rat liver decreased, and the liver pathological morphology was restored to normal after treatment with PC extract. At the same time, HE staining on the liver illustrated that HFD feeding induced fat cavities and liver cell turbidity (which was showed by arrows) in the liver tissue after 12 weeks, which was reversed by PC extract treatment (Fig. 5B). Furthermore, the TC, TG, ALT, AST, and LDL-C levels were significantly increased ($P < 0.001$), and the HDL-C level showed a downward trend after 12 weeks of HFD-feeding (Fig. 5D–I). However, after treatment with PC extract, the TG, ALT, and AST levels were significantly decreased ($P < 0.05$, $P < 0.001$), the HDL-C level was significantly increased ($P < 0.01$, $P <$

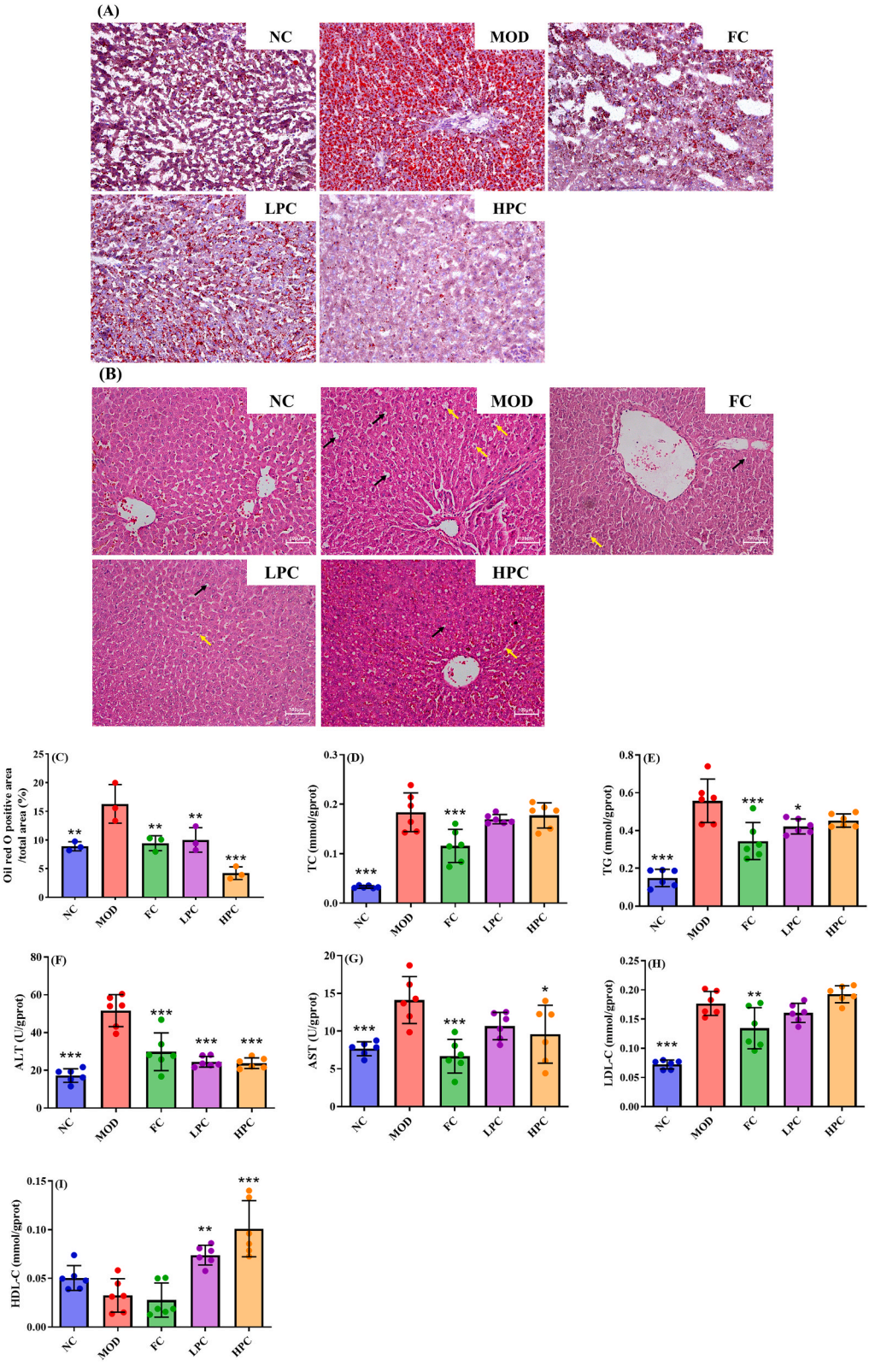

(caption on next page)

Fig. 5. Effects of PC extract on liver lipid contents of HFD-fed rats. Liver histology after oil red O staining (A) and HE staining (B) in which the black arrows indicate macrovesicular steatosis and yellow arrows indicate ballooning of hepatocytes. Quantitative analysis of oil red O positive area in the liver (C). Levels of (D) TC, (E) TG, (F) ALT, (G) AST, (H) LDL-C, and (I) HDL-C in the liver. $^{*}P < 0.05$, $^{**}P < 0.01$, $^{***}P < 0.001$ vs. MOD group. ALT, alanine transaminase; AST, aspartate transaminase; FC, fenofibrate control group; HDL-C, high density lipoprotein cholesterol; HE, hematoxylin and eosin; HFD, high-fat diet; HPC, high-dose of *poria cocos* extract; LDL-C, low density lipoprotein cholesterol; LPC, low-dose of *poria cocos* extract; MOD, model group; NC, normal control group; TC, total cholesterol; TG, triglyceride.

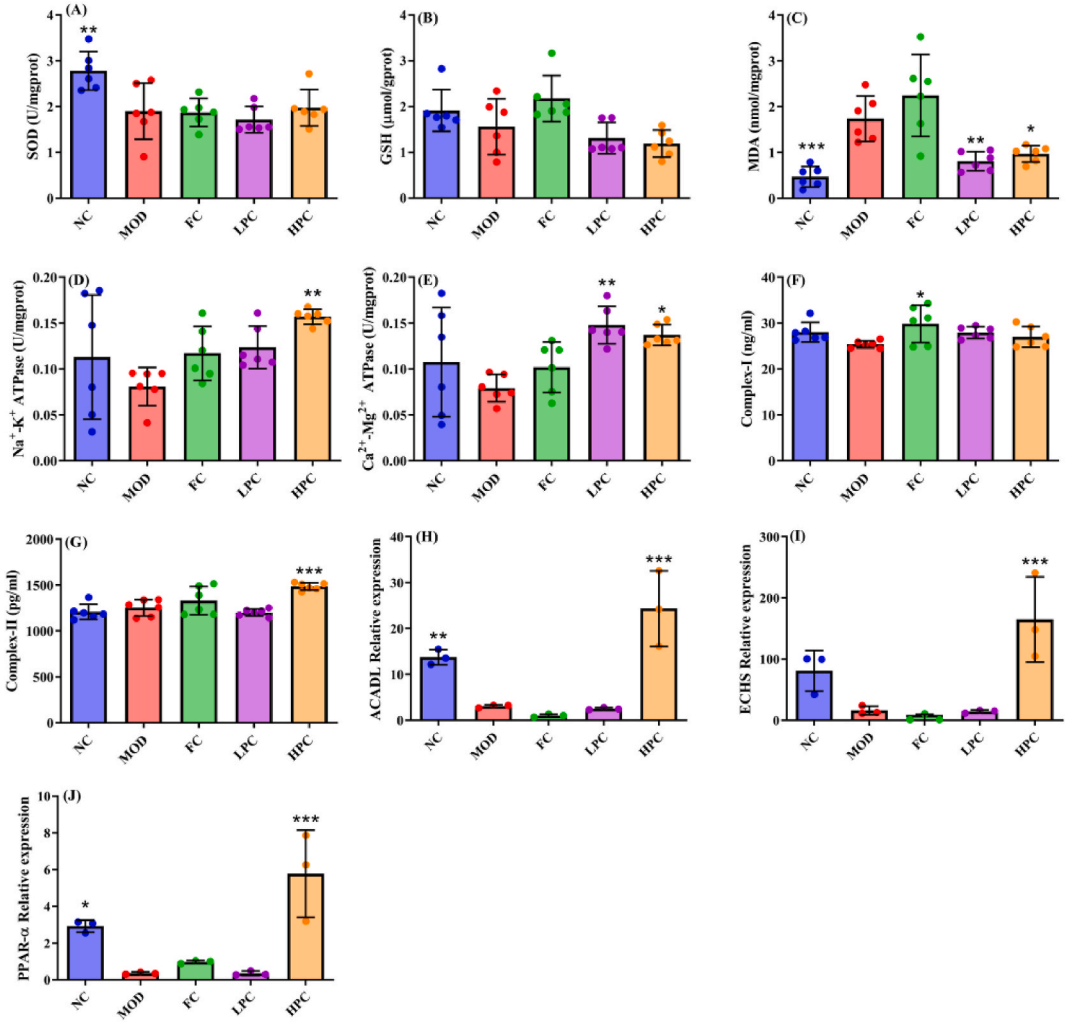

Fig. 6. Effects of PC extract on the mitochondrial status of liver from HFD-fed rats. Levels of (A) SOD; (B) GSH; (C) MDA; (D) Na^{+}-K^{+}-ATPase, (E) Ca^{2+}-Mg^{2+}-ATPase, (F) Complex-I, and (G) Complex-II in isolated liver mitochondria. mRNA expression levels of (H) ACADL, (I) ECHS, and (J) PPAR-α in isolated liver mitochondria. $^{*}P < 0.05$, $^{**}P < 0.01$, $^{***}P < 0.001$ vs. MOD group. ACADL, long chain Acyl-coenzyme A dehydrogenase; ATPase, ATP synthase; Complex-I/II: rats mitochondrial respiratory chain complex I and II; ECHS, short chain Enoyl-coenzyme A hydratase; FC, fenofibrate control group; GSH, glutathione; HPC, high-dose of *poria cocos* extract; LPC, low-dose of *poria cocos* extract; MDA, malondialdehyde; MOD, model group; NC, normal control group; PPAR-α, peroxisome proliferator activated receptor α; SOD, superoxide dismutase.

0.001), and the TC and LDL-C levels were not significantly affected. These findings suggest that PC extracts alleviated lipid abnormalities and damage in the liver of HFD-fed rats.

3.2.3. *Effects PC extract on mitochondrial status*

After 12 weeks of HFD-feeding, the SOD and MDA levels were significantly decreased and increased in the liver mitochondria, respectively ($P < 0.05$, $P < 0.01$). At the same time, the GSH, ATPase, and Complex-I levels showed a downward trend, and the Complex-II level was not significantly affected (Fig. 6A–G). However, treatment with PC extract significantly decreased the MDA level ($P < 0.05$, $P < 0.01$). and significantly increased the Na^{+}-K^{+}-ATPase, Ca^{2+}-Mg^{2+}-ATPase, Complex-II levels ($P < 0.05$, $P < 0.01$, $P <$ 0.001). Additionally, the Complex-I level showed an upward trend, and the levels of SOD and GSH were not affected significantly.

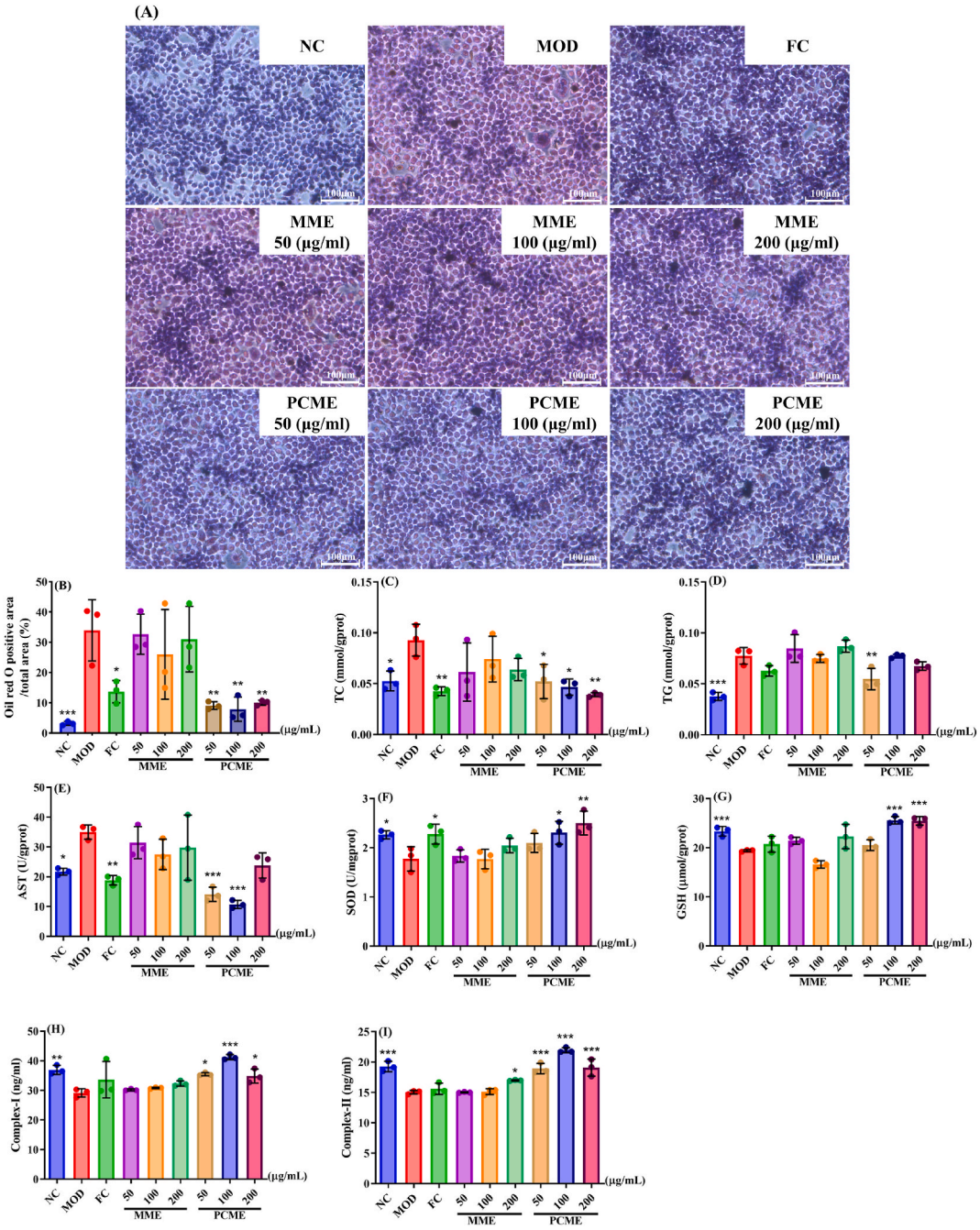

Fig. 7. Effects of PC-derived ingredients in liver mitochondria on fat emulsion-induced L02 adipocytes. Fat accumulation in cells after oil red O staining (A). Quantitative analysis of oil red O positive area in cells (B). Cellular (C) TC; (D) TG; (E) AST; (F) SOD; (G) GSH; (H) Complex-I; and (I) Complex-II levels. Data represent the average of three independent measurements. $^{*}P < 0.05$, $^{**}P < 0.01$, $^{***}P < 0.001$ vs. MOD group. AST, aspartate transaminase; Complex-I/II: mitochondrial respiratory chain complex I and II; FC, fenofibrate control group; GSH, glutathione; MOD, model group; MME, liver mitochondrial extract of model group; NC, normal control group; PCME, liver mitochondrial extract of high-dose of PC extract; SOD, superoxide dismutase; TC, total cholesterol; TG, triglyceride.

These results suggest that the PC extract promoted the mitochondrial function, relieving MAFLD.

HFD-feeding for 12 weeks significantly decreased the mRNA expressions of the long-chain Acyl-coenzyme A dehydrogenase (ACADL) and peroxide proliferator-activated receptor α (PPAR-α) ($P < 0.05$, $P < 0.01$). On the contrary, the short-chain Enoyl-coenzyme A hydratase (ECHS) showed a downward trend (Fig. 6H–J). However, treatment with the PC extract significantly increased the ACADL, ECHS, and PPAR-α mRNA expressions ($P < 0.001$), implying that the PC extract stimulated fatty acid β oxidation to alleviate

Table 5
UHPLC/MS data and structure assignment of PC-derived chemicals from liver mitochondria.

NO.	t_R	$[M+H]^+$ $[M+Na]^+$ m/z	ESI-MS^2(+) m/z (abundance)	$[M-H]^-$m/z	ESI-MS^2(−) m/z(abundance)	Predicted formula	Predicted (m/z)	Measured (m/z)	Diff (ppm)	Assigned identification
1	7.3009			349.1995	265(42)	$C_{21}H_{34}O_4$	349.1975	349.1995	5.59	Pregn-7-ene-2β,3α,15α,20(s)-tetrol [16]
2	41.3442			571.3627	617(43), 509(38), 507(18), 429(1)	$C_{34}H_{52}O_7$	571.3613	571.3627	2.39	3β,16α-Bis(acetyloxy)-29-hydroxylanosta-8,24-dien-21-oic acid [17]
3[a]	41.9280			471.3481	409(29), 275(22), 407(3), 337(7), 207(3), 453(11), 427(3)	$C_{30}H_{48}O_4$	471.3482	471.3481	−0.24	16α-Hydroxytrametenolic acid [16,18]
4[a]	43.5626			485.3202	325(25), 387(20), 441(3), 553(10), 531(5), 467(12)	$C_{30}H_{46}O_5$	485.3176	485.3202	5.31	Poricoic acid G [17,19,20]
5	54.5880			543.3615	525(32), 494(7)	$C_{33}H_{52}O_6$	543.3686	543.3615	−13.07	Hydroxypachymic acid [20]
6	55.9890			559.3641	627(11), 515(15)	$C_{33}H_{52}O_7$	559.3672	559.3641	−5.67	25-Methoxy-29-hydroxyporicoic acid HM [17]
7	57.5569			543.3334	447(22), 429(10), 467(31), 451(10), 481(5), 525(12), 465(20), 421(29)	$C_{32}H_{48}O_7$	543.3341	543.3334	−1.31	26-Hydroxyporicoic acid DM [18,21]
8	59.4584			501.3209	439(24)	$C_{30}H_{46}O_6$	501.3197	501.3209	2.46	26-Hydroxy-poricoic acid G [22]
9	20.4868	501.3189	465(8), 485(9), 357 (6), 325(14)			$C_{30}H_{44}O_6$	501.3167	501.3189	4.36	Poricoic acid E [23]
10[a]	35.1149	527.3707	483(97), 449(3)			$C_{33}H_{50}O_5$	527.3683	527.3707	4.47	Dehydropachymic acid [23]
11[a]	37.7503	483.3469	483(63), 99(23), 447 (8), 965(4)			$C_{31}H_{46}O_4$	483.3469	483.3469	−0.04	Polyporenic acid C [23,24]
12[a]	38.8512	467.3545	323(20), 421(1), 309 (1)			$C_{31}H_{46}O_3$	467.3570	467.3545	−5.32	Dehydroeburiconic acid [23]
13[a]	40.7693	485.3600	485(100), 467(2), 449(4), 453(2)			$C_{31}H_{48}O_4$	485.3575	485.3600	5.18	Dehydrotumulosic acid [25]
14	43.755	469.3666	469(60), 293(57), 423(49)			$C_{31}H_{48}O_3$	469.3656	469.3666	2.16	Dehydroeburicoic acid [23,25]
15[a]	45.7066	455.3537	967(13), 485(11)			$C_{30}H_{46}O_3$	455.3555	455.3537	−3.87	Dehydrotrametenolic acid [24]

[a] Compared with reference substances.

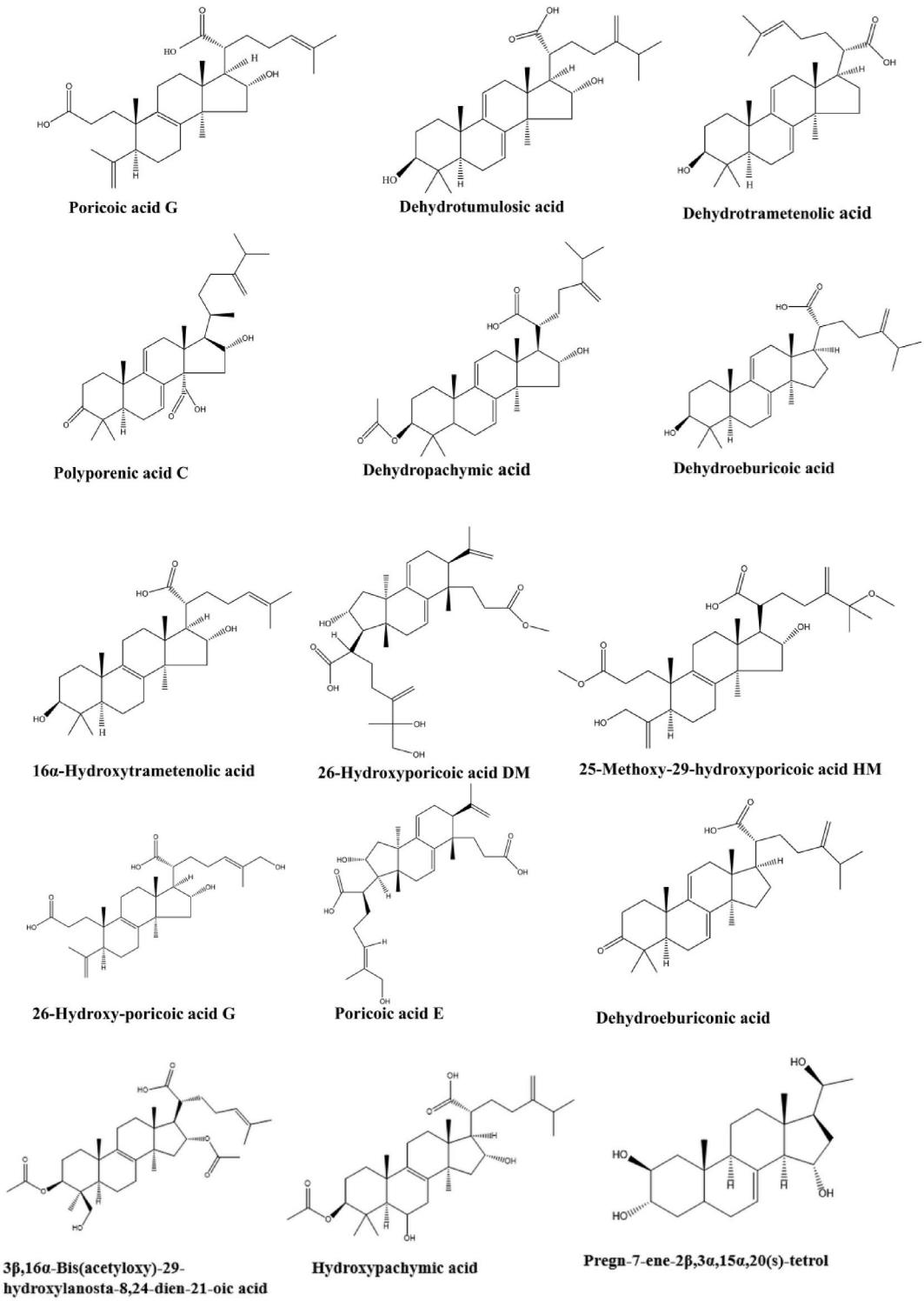

Fig. 8. Chemical structures of PC-derived ingredients derived from the liver mitochondria extract.

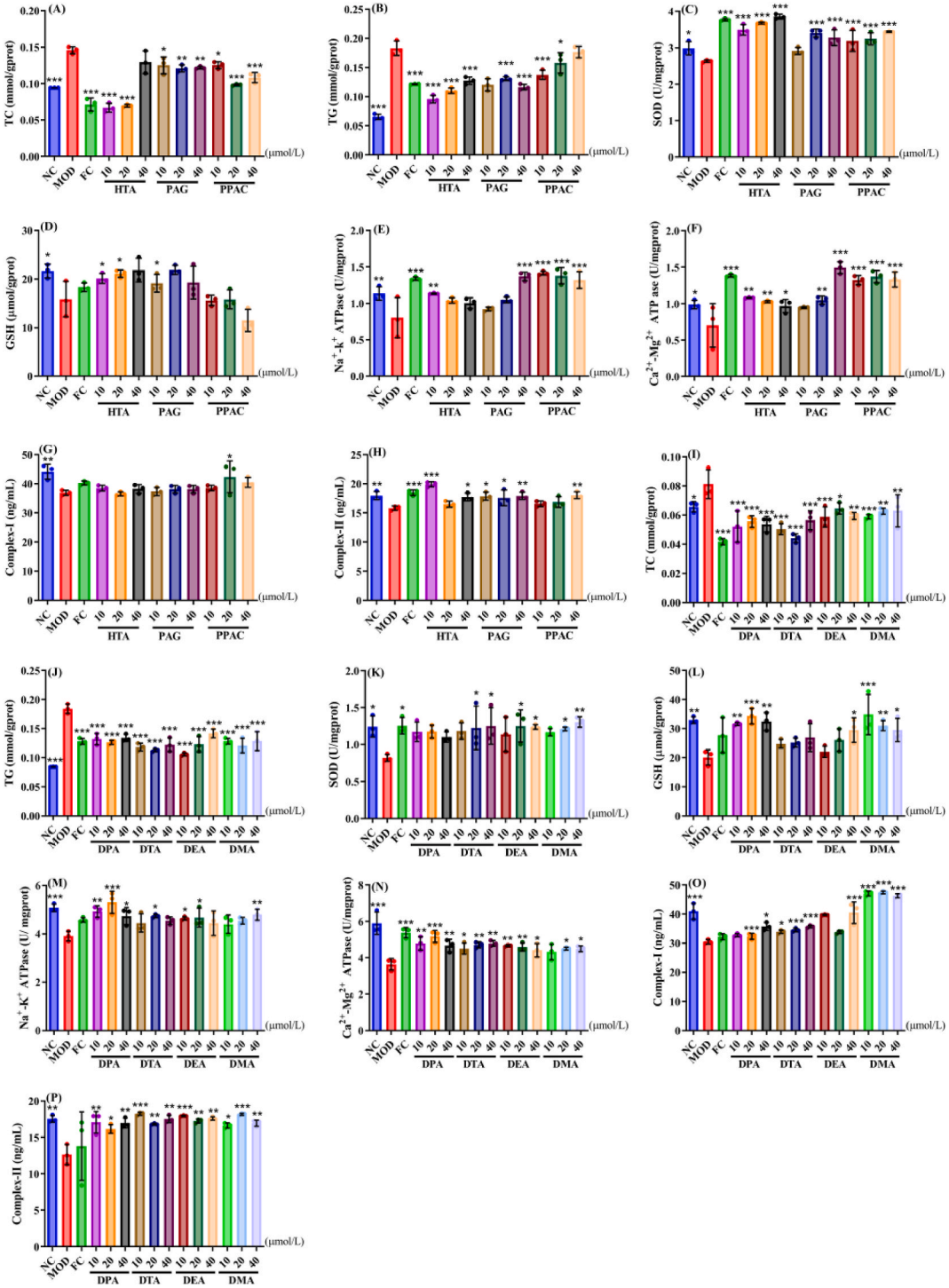

Fig. 9. Effects of PC-derived chemicals from the liver mitochondria on fat emulsion-induced L02 adipocytes. Cellular (A and I) TC; (B and J) TG; (C and K) SOD; (D and L) GSH; (E and M) Na^{+}-K^{+}-ATPase; (F and N) Ca^{2+}-Mg^{2+}-ATPase; (G and O) Complex-I; and (H and P) Complex-II levels Data represent the average of three independent measurements. $^{*}P < 0.05$, $^{**}P < 0.01$, $^{***}P < 0.001$ vs. MOD group. ATPase, ATP synthase; Complex-I/II: mitochondrial respiratory chain complex I/II; DEA, Dehydroeburicoic acid; DMA, Dehydrotrametenolic acid; DPA, Dehydropachymic acid; DTA, Dehydrotumulosic acid; FC, fenofibrate control group; GSH, glutathione; HTA, 16α-Hydroxytrametenolic acid; MOD, model group; NC, normal control group; PAG, Poricoic acid G; PPAC, Polyporic acid C; SOD, superoxide dismutase; TC, total cholesterol; TG, triglyceride.

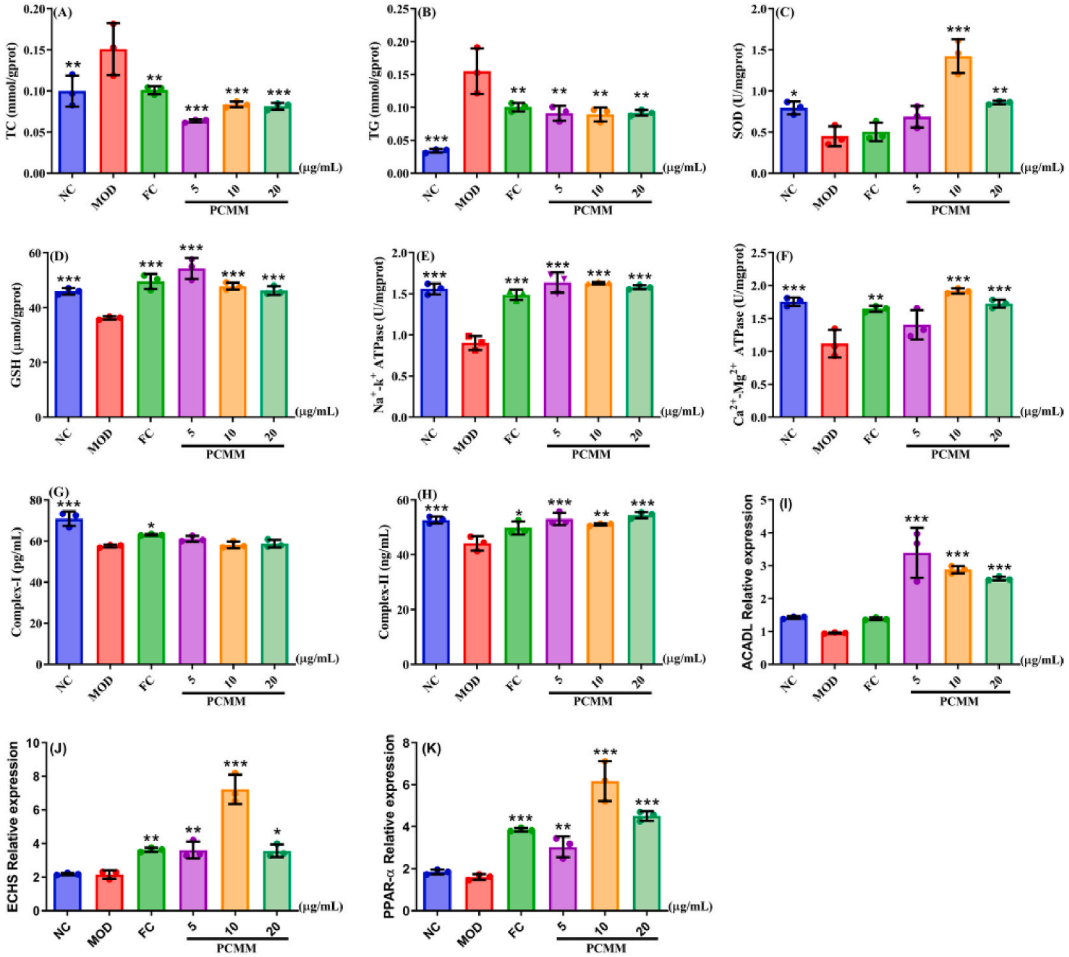

Fig. 10. Effects of PC-derived chemical group from the liver mitochondria on fat emulsion-induced L02 adipocytes. Cellular levels of (A) TC; (B) TG; (C) SOD; (D) GSH; (E) Na^{+}-K^{+}-ATPase; (F) Ca^{2+}-Mg^{2+}-ATPase; (G) Complex-I; and (H) Complex-II. The mRNA expression levels of (I) CPT-1B, (J) UCP-2, and (K) FAS in the emulsion-induced L02 adipocytes. Data represent the average of three independent measurements. $^{*}P < 0.05$, $^{**}P < 0.01$, $^{***}P < 0.001$ vs. MOD group. ATPase, ATP synthase; Complex I/II, mitochondrial respiratory chain complex I/II; CPT-1 B, carnitine palmitoyltransferase 1 B; FAS, fatty acid synthase; FC, fenofibrate control group; GSH, glutathione; MOD, model group; NC, normal control group; PCMM, PC-derived monomers group in mitochondria; qRT-PCR, quantitative real-time PCR; SOD, superoxide dismutase; TC, total cholesterol; TG, triglyceride; UCP-2, uncoupling protein 2.

liver fatty degeneration in HFD-fed rats.

3.3. *Effects of PC-derived ingredients from the liver mitochondria on adipocytes*

Fat emulsion stimulation increased intracellular lipid levels (Fig. 7A and B). However, after PCME treatment, intracellular lipid accumulation was significantly inhibited. On the contrary, MME treatment failed to inhibit lipid accumulation. Nonetheless, fat emulsion stimulation significantly increased the TC, TG, and AST levels ($P < 0.05$, $P < 0.001$), and decreased the GSH, SOD, Complex-I, and Complex-II levels ($P < 0.05$, $P < 0.01$, $P < 0.001$) (Fig. 7C–I). Interestingly, PCME treatment significantly decreased the TC, TG, and AST levels ($P < 0.05$, $P < 0.01$, $P < 0.001$), and significantly increased the GSH, SOD, and Complex-I/II levels ($P < 0.05$, $P < 0.01$, $P < 0.001$). However, treatment with MME did not alter the fat emulsion-induced pathological changes except for a significant reversal of the Complex-II level. These results suggest that PC-derived ingredients from the liver mitochondrial extracts remediate oxidative stress and energy metabolism, alleviating cellular steatosis.

A comparison of the accurate high-resolution MS^{n} data provided by UHPLC/MS (Table 5) and previously reported data [16–25] identified fifteen PC-derived chemicals, including fourteen prototype chemicals and one metabolite (whose prototype was pachymic acid) were identified from the PC-treated rat liver mitochondrial extracts (Fig. 8). Among the identified chemicals, there were fourteen triterpene acids and one sterol.

3.4. Effects of PC-derived components and component group from the mitochondria on adipocytes

The TC, and TG levels were significantly increased ($P < 0.001$), and the GSH, SOD, Na^+-K^+-ATPase, Ca^{2+}-Mg^{2+}-ATPase, Complex-I, and Complex-II were significantly decreased ($P < 0.05$, $P < 0.01$, $P < 0.001$) after 24 h of stimulation with fat emulsion (Fig. 9). However, the TC and TG levels were significantly reduced ($P < 0.05$, $P < 0.01$, $P < 0.001$), and the SOD, GSH, Na^+-K^+-ATPase, Ca^{2+}-Mg^{2+}-ATPase and Complex-II levels were significantly increased ($P < 0.05$, $P < 0.01$, $P < 0.001$) after treatment with HTA or PAG. Additionally, the Complex-I levels showed an upward trend. At the same time, TC and TG levels were significantly reduced ($P < 0.05$, $P < 0.001$), the SOD, Na^+-K^+-ATPase, Ca^{2+}-Mg^{2+}-ATPase, Complex-I, and Complex-II levels were significantly increased ($P < 0.05$, $P < 0.01$, $P < 0.001$), and the GSH level showed an upward trend after treatment with PPAC. DPA treatment significantly reduced the TC and TG levels ($P < 0.001$), significantly increased the GSH, Na^+-K^+-ATPase, Ca^{2+}-Mg^{2+}-ATPase, Complex-I and Complex-II levels ($P < 0.05$, $P < 0.01$, $P < 0.001$), and induced an upward trend in the SOD levels. Similarly, DTA treatment significantly reduced the TC and TG levels ($P < 0.001$). However, it significantly increased the SOD, Na^+-K^+-ATPase, Ca^{2+}-Mg^{2+}-ATPase, Complex-I and Complex-II levels ($P < 0.05$, $P < 0.01$, $P < 0.001$). Besides, the GSH level showed an upward trend following DTA treatment. On the contrary, DEA and DMA treatment significantly reduced the TC and TG levels ($P < 0.05$, $P < 0.01$, $P < 0.001$). At the same time, DEA and DMA treatment significantly increased the SOD, GSH, Na^+-K^+-ATPase, Ca^{2+}-Mg^{2+}-ATPase, Complex-I, and Complex-II levels ($P < 0.05$, $P < 0.01$, $P < 0.001$). These results suggest that PC-derived components regulated oxidative stress and energy metabolism in steatosis hepatocytes to reduce lipid accumulation.

Moreover, treatment with PCMM significantly reduced the TC and TG levels ($P < 0.01$, $P < 0.001$) and increased the SOD, GSH, Na^+-K^+-ATPase, Ca^{2+}-Mg^{2+}-ATPase, and Complex-II levels ($P < 0.01$, $P < 0.001$), with an upward Complex-I upward trend (Fig. 10A–H). These results suggest that oxidative stress and energy metabolism were improved by PCMM, further alleviating cell steatosis. Additionally, stimulation with fat emulsion decreased the mRNA expression levels of ACADL, ECHS, and PPAR-α in cells but was reversed by PCMM treatment ($P < 0.05$, $P < 0.01$, $P < 0.001$) (Fig. 10I–K) implying that PCMM regulated the gene expression levels of fatty acid β oxidation-related genes to alleviate steatosis.

4. Discussion

L02 adipocyte and MAFLD rat models induced by fat emulsion and HFD, respectively, were used to explore the efficacy of PC against MAFLD [26]. PC reduced TG, TC, ALT, and AST levels and accumulation of lipid droplets in L02 cells induced by fat emulsion. Moreover, PC decreased TG, TC, ALT, LDL-C, and AST levels in the serum and liver, increased HDL-C levels in the liver, and reduced body weight and hepatomegaly in rats with high-fat diet-induced MAFLD. PC also alleviated the histopathological abnormalities and reduced the formation and accumulation of lipid droplets in the liver. These findings suggest that PC effectively reverses lipid metabolism disorder in rats with HFD-induced MAFLD.

Mitochondria are “cell power plants” and key metabolic organelles. MAFLD occurrence and development in the liver mitochondria is accompanied by energy metabolism disorder [27], decreased ATPase and mitochondrial respiratory chain complexes I and II, and hepatocyte mitochondria ultrastructural changes [26]. In addition, mitochondrial dysfunction produces excess ROS and MDA, accelerating oxidative stress. ROS are highly toxic molecules detoxified by the antioxidant system. As detoxifying enzymes, SOD and GSH protect biomolecules and cell structures from ROS damage. However, MDA, SOD, and GSH are imbalanced in the mitochondria of MAFLD rat model [28,29]. In the present study, PC treatment significantly increased the SOD, GSH, ATPase, and Complex-I levels in the liver L02 cells mitochondria, reduced the mitochondrial damage in L02 cells, and improved the mitophagy level in L02 cells. PC also significantly increased the ATPase and Complex-II activities and decreased the MDA level in rat liver mitochondria. These results indicate that PC improved mitophagy and alleviated the energy metabolism disorder and oxidative stress damage in the liver, mitigating the MAFLD symptoms in the rats.

In addition, impaired mitochondrial fatty acid oxidation plays a major role in the occurrence and development of MAFLD [30]. ACADL is a mitochondrial enzyme that catalyzes the initial step of fatty acid oxidation [31]. PPAR-α is a transcription regulatory gene involved in the peroxisome, mitochondrial β oxidation, fatty acid transport, and hepatic glucose production. Activated PPAR-α prevents fatty accumulation, liver inflammation, and fibrosis [32]. Besides, the ECHS overexpression, a key metabolic enzyme catalyzing the β oxidation of mitochondrial fatty acid, reduces steatosis, inflammation, fibrosis, apoptosis, and oxidative stress [33]. Fatty acids are generally absorbed into the cytoplasm through CD 36, fatty acid transporters, and fatty acid binding proteins and then transported to the mitochondria by CPT-1 B for β oxidation [26]. FAS catalyzes the *de novo* synthesis of fatty acids, which regulates the expression of lipogenesis-related genes and the activation of PPAR-α, a major transcription factor related to fatty acid homeostasis [34].

Moreover, the overexpression of UCP-2 decreases the production of mitochondrial ATP, inhibiting the fatty acid β oxidation function [35,36]. In this study, PC significantly up-regulated the CPT-1B mRNA expression and decreased that of FAS and UCP-2 mRNA in L02 cells. PC also significantly up-regulated ECHS, PPAR, and ACADL mRNA levels in the liver of the MAFLD rat model. These results indicate that PC regulated the expression of β-oxidation-related genes, alleviating MAFLD.

The ‘mitochondrial pharmacology and pharmacochemistry’ strategy effectively identifies the main TCMs active components that regulate mitochondrial function and prevent human diseases [13]. This study used this strategy to uncover the active substances in PC that regulate mitochondrial function and alleviate MAFLD. Mitochondrial pharmacology revealed that PC-derived components in MAFLD rat model liver mitochondria alleviated the lipid metabolism disorder in liver L02 cells induced by medicinal fat emulsion by attenuating the oxidative stress injury and improving the energy metabolism. Furthermore, 15 PC-derived chemicals, including fourteen prototype components (HTA, PAG, DMA, DTA, DPA, DEA, PPAC, Pregn-7-ene-2β, 3α, 15α, 20 (s)-tetrol, 26-Hydroxyporicoic acid DM, 3β,16α-Bis(acetyloxy)-29-hydroxylanosta-8,24-dien-21-oic acid, 25-Methoxy-29-hydroxyporicoic acid HM,

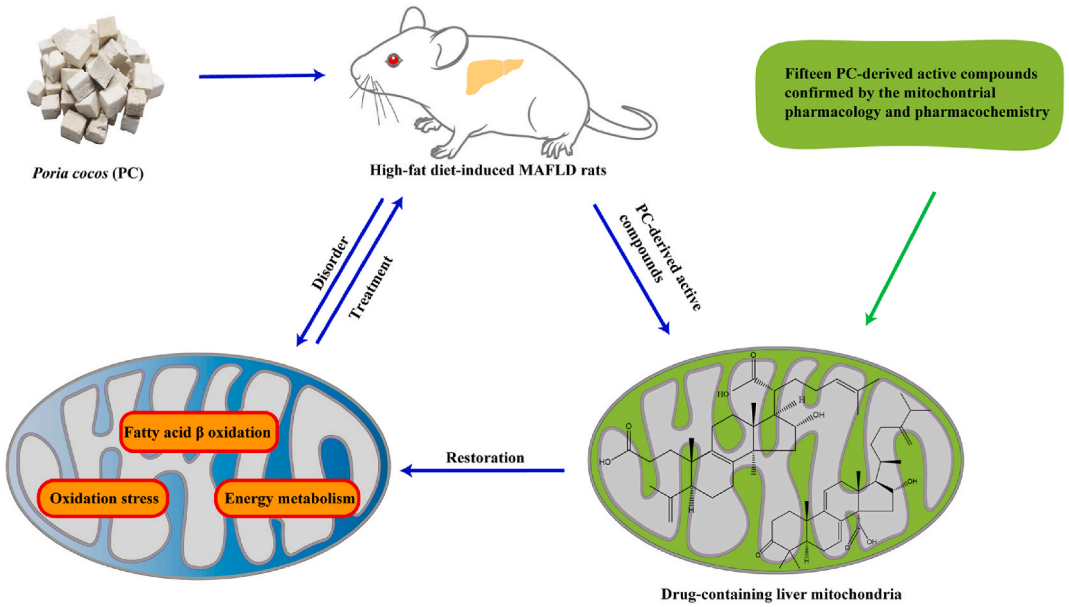

Fig. 11. PC extract regulated HFD-induced MAFLD by remedying mitochondrial functions. The fifteen ingredients identified from liver mitochondria are potentially the main effective compounds of PC against MAFLD. HFD, high-fat diet; MAFLD, metabolic dysfunction associated fatty liver; PC, *Poria cocos*.

26-Hydroxy-poricoic acid G, Dehydroeburiconic acid, Poricoic acid E), and one metabolite (Hydroxypachymic acid) that entered the MAFLD rat model mitochondria treated with PC extract were successfully confirmed by mitochondrial pharmacochemistry.

Among the 15 compounds identified from PC-treated rat liver mitochondria, DMA [37] can be used as an insulin sensitizer in obese hyperglycemic db/db mice. DTA and PPAC reduce lipid levels by inhibiting bile acid uptake transporters within the enterohepatic circulation [38]. DEA [39] has the capability of alleviating hyperlipidemia, with the potential to enhance AMPK activity and PPAR-α expression while decreasing FAS expression. In this study, seven PC-derived monomers (HTA, PAG, DMA, DTA, DPA, DEA, and PPAC) decreased the TC, TG, ALT, and AST levels and increased the SOD, GSH, ATP, Complex-I, and Complex-II levels in hepatocytes. In addition, the PC-derived monomer group composed of HTA, PAG, DMA, DTA, DPA, DEA, and PPAC reduced the TC and TG levels and increased the SOD, GSH, ATPase, Complex-I and Complex-II levels, and the expression of ACADL, ECHS, and PPAR- α mRNA in hepatocytes. These results demonstrate that the nine compounds are potential bioactive components regulating mitochondria function to alleviate dyslipidemia, suggesting that mitochondrial pharmacology and pharmacochemistry results are reliable. The other six identified compounds are potential bioactive molecules remedying mitochondria to alleviate dislipidemia that require further investigation. Overall, these findings suggest that identified chemical compounds are potential active components of PC, with the capacity to alleviate HFD-induced MAFLD.

5. Conclusion

PC extract effectively alleviates the lipid metabolism disorder associated with MAFLD by restoring the mitochondria ultrastructure and function (Fig. 11). The mitochondria ultrastructure and function are restored by reduced oxidative stress injury, enhanced energy metabolism, and regulating the fatty acid β oxidation. Besides, the main PC pharmacological components regulating mitochondria to alleviate MAFLD consisted of 15 chemicals. Overall, PC has the potential for use as a medicine/nutrient to repair mitochondria and alleviate MAFLD.

Ethics declarations

Animal Ethics Committee of the Institute of Yunnan University of Chinese Medicine, No. R-062021G103.

Data availability statement

Data will be made available on request.

Funding

This study was supported by grants from the National Natural Science Foundation of China (Grants 82104381, 82060707,

82160748, 82174037, and 81960710), the Application and Basis Research Project of Yunnan China (Grants 202201AW070016, 202301AS070070, 202001AZ070001–006, 202001AZ070001–043, and 202001AV070007), and the Young and Middle-aged Academic and Technological Leader of Yunnan (Grant 202005AC160059).

CRediT authorship contribution statement

Yanjuan Li: Writing – review & editing, Writing – original draft, Methodology, Investigation. **Pengquan Wang:** Writing – review & editing, Data curation. **Huan Yang:** Investigation, Data curation. **Jinbiao He:** Investigation. **Yu Yang:** Investigation. **Yuxuan Tao:** Validation. **Min Zhang:** Validation. **Mei Zhang:** Writing – review & editing. **Jie Yu:** Resources, Project administration. **Xingxin Yang:** Supervision, Project administration, Funding acquisition.

Declaration of competing interest

The authors declare that they have no known competing financial interests or personal relationships that could have appeared to influence the work reported in this paper.

References

[1] S. Pouwels, N. Sakran, Y. Graham, A. Leal, T. Pintar, W. Yang, R. Kassir, R. Singhal, K. Mahawar, D. Ramnarain, Non-alcoholic fatty liver disease (NAFLD): a review of pathophysiology, clinical management and effects of weight loss, BMC Endocr. Disord. 22 (2022) 63, https://doi.org/10.1186/s12902-022-00980-1.
[2] E. Cobbina, F. Akhlaghi, Non-alcoholic fatty liver disease (NAFLD) - pathogenesis, classification, and effect on drug metabolizing enzymes and transporters, Drug Metab. Rev. 49 (2017) 197–211, https://doi.org/10.1080/03602532.2017.1293683.
[3] M.P. Pathak, K. Pathak, R. Saikia, U. Gogoi, P. Patowary, P. Chattopadhyay, A. Das, Therapeutic potential of bioactive phytoconstituents found in fruits in the treatment of non-alcoholic fatty liver disease: a comprehensive review, Heliyon 9 (4) (2023) e15347. https://do-i.org/10.1016/j.heliyon.2023.e15347.
[4] A. Mantovani, A. Dalbeni, Treatments for NAFLD: state of art, Int. J. Mol. Sci. 22 (2021) 2350, https://doi.org/10.3390/ijms22052350.
[5] X. Hu, T. Duan, Z. Wu, Y. Xiong, Z. Cao, Intercellular mitochondria transfer: a new perspective for the treatment of metabolic diseases, Acta Biochim. Biophys. Sin. 53 (2021) 958–960, https://doi.org/10.1093/abbs/gmab052.
[6] A. Mansouri, C.H. Gattolliat, T. Asselah, Mitochondrial dysfunction and signaling in chronic liver diseases, Gastroenterology 155 (2018) 629–647, https://doi.org/10.1053/j.gastro.201-8.06.083.
[7] L. Wu, W. Mo, J. Feng, J. Li, Q. Yu, S. Li, J. Zhang, K. Chen, J. Ji, W. Dai, J. Wu, X. Xu, Y. Mao, C. Guo, Astaxanthin attenuates hepatic damage and mitochondrial dysfunction in non-alcoholic fatty liver disease by up-regulating the FGF21/PGC-1α pathway, Br. J. Pharmacol. 177 (2020) 3760–3777, https://doi.org/10.1111/bph.15099.
[8] X.X. Yang, X. Wang, T.T. Shi, J.C. Dong, F.J. Li, L.X. Zeng, M. Yang, W. Gu, J.P. Li, J. Yu, Mitochondrial dysfunction in high-fat diet-induced nonalcoholic fatty liver disease: the alleviating effect and its mechanism of Polygonatum kingianum, Biomed. Pharmacother. 117 (2019) 109083, https://doi.org/10.1016/j.biopha.2019.109083.
[9] M.Y. Song, S.Y. Kang, A. Kang, J.H. Hwang, Y.K. Park, H.W. Jung, Cinnamomum cassia prevents high-fat diet-induced obesity in mice through the increase of muscle energy, Am. J. Chin. Med. 45 (2017) 1017–1031, https://doi.org/10.1142/S0192415X17500549.
[10] J.H. Kim, H.A. Sim, D.Y. Jung, E.Y. Lim, Y.T. Kim, B.J. Kim, M.H. Jung, *Poria cocus* wolf extract ameliorates hepatic steatosis through regulation of lipid metabolism, inhibition of ER stress, and activation of autophagy via AMPK activation, Int. J. Mol. Sci. 20 (2019) 4801, https://doi.org/10.3390/ijms20194801.
[11] J.L. Ríos, Chemical constituents and pharmacological properties of *Poria cocos*, Planta Med. 77 (2011) 681–691, https://doi.org/10.1055/s-0030-1270823.
[12] J. He, Y. Yang, F. Zhang, Y. Li, X. Li, X. Pu, X. He, M. Zhang, X. Yang, Q. Yu, Y. Qi, X. Li, J. Yu, Effects of *Poria cocos* extract on metabolic dysfunction-associated fatty liver disease *via* the FXR/PPARα-SREBPs pathway, Front. Pharmacol. 13 (2022) 1007274, https://doi.org/10.3389/fphar.2022.1007274.
[13] L.P. Yu, Y.Q. Li, Y.J. Li, L. Zi, Y.X. Tao, J.J. Hao, M. Zhang, W. Gu, F. Zhang, J. Yu, X.X. Yang, In vivo identification of the pharmacodynamic ingredients of *Polygonum cuspidatum* for remedying the mitochondria to alleviate metabolic dysfunction-associated fatty liver disease, Biomed. Pharmacother. 156 (2022) 113849, https://doi.org/10.1016/j.biopha.2022.11-3849.
[14] Y. Yang, X.L. Huang, Z.M. Jiang, X.F. Li, Y. Qi, J. Yu, X.X. Yang, M. Zhang, Quantification of chemical groups and quantitative HPLC fingerprint of *Poria cocos* (schw.) wolf, Molecules 27 (2022) 6383, https://doi.org/10.3390/molecules27196383.
[15] X.S. Jiang, J. Dai, Q.H. Sheng, L. Zhang, Q.C. Xia, J.R. Wu, R. Zeng, A comparative proteomic strategy for subcellular proteome research: ICAT approach coupled with bioinformatics prediction to ascertain rat liver mitochondrial proteins and indication of mitochondrial localization for catalase, Mol. Cell. Proteomics 4 (2005) 12–34, https://doi.org/10.1074/mc-p.M400079-MCP200.
[16] M. Yang, Y. Zhao, Y. Qin, R. Xu, Z. Yang, H. Peng, Untargeted metabolomics and targeted quantitative analysis of temporal and spatial variations in specialized metabolites accumulation in *Poria cocos* (schw.) wolf (fushen), Front. Plant Sci. 12 (2021) 713490, https://doi.org/10.3389/fpls.2021.713490.
[17] Y.T. Zou, F. Long, C.Y. Wu, J. Zhou, W. Zhang, J.D. Xu, Y.Q. Zhang, S.L. Li, A dereplication strategy for identifying triterpene acid analogues in Poria cocos by comparing predicted and acquired UPLC-ESI-QTOF-MS/MS data, Phytochem. Anal. 30 (2019) 292–310, https://doi.org/10.1002/pca.2813.
[18] G.F. Feng, Y. Zheng, Y. Sun, S. Liu, Z.F. Pi, F.R. Song, Z.Q. Liu, A targeted strategy for analyzing untargeted mass spectral data to identify lanostane-type triterpene acids in *Poria cocos* by integrating a scientific information system and liquid chromatography-tandem mass spectrometry combined with ion mobility spectrometry, Anal. Chim. Acta 1033 (2018) 87–99, https://doi.org/10.1016/j.aca.2018.06.048.
[19] H.R. Li, P.P. Dong, H.J. Li, J. Xu, H. Wang, Y.F. Cui, Z.Q. Sun, P. Gao, J.Y. Zhang, [UHPLC-Q-Exactive Orbitrap MS/MS-based rapid identification of chemical components in substance benchmark of Kaixin San], Zhongguo Zhongyao Zazhi 4 (2022) 938–950.
[20] J.T. Liu, Y. Zhang, R.Z. Bu, H.P. Zhao, Y. Zhao, H.B. Zhang, J. Xu, T.J. Zhang, L. Wang, C.X. Liu, Indentification of chemical components and blood components of Biqi Capsules by UPLC-Q/TOF-MS, Chin. Tradit. Herbal Drugs 18 (2021) 5496–5513.
[21] A. Kang, J.R. Guo, T. Xie, J.J. Shan, L.Q. Di, Analysis of the triterpenes in poria cocos by UHPLC-LTQ-orbitrap MS/MS, J. Nanjing univ. Tradit, Chin. Med. 6 (2014) 561–565.
[22] W. Wang, H. Dong, R. Yan, H. Li, P. Li, P. Chen, B. Yang, Z. Wang, Comparative study of lanostane-type triterpene acids in different parts of *Poria cocos* (Schw.) Wolf by UHPLC-Fourier transform MS and UHPLC-triple quadruple MS, J. Pharm. Biomed. Anal. 102 (2015) 203–214, https://doi.org/10.1016/j.jpba.2014.09.014.
[23] X. Fang, X.P. Ding, L.L. Chen, J.F. Zan, H.D. Shen, A.N. Hu, J.F. Liu, Analysis of triterpenoids in peels of Poria cocos by HPLC-LTQ-Orbitrap-MS, Lishizhen Med. Materia Medica Res. 30 (2019) 2117–2121.
[24] Y. Zhang, Y. Cheng, Z. Liu, L. Ding, T. Qiu, L. Chai, F. Qiu, Z. Wang, W. Xiao, L. Zhao, X. Chen, Systematic screening and characterization of multiple constituents in Guizhi Fuling capsule and metabolic profiling of bioactive components in rats using ultra-high-performance liquid chromatography/quadrupole-time-of-flight mass spectrometry, J. Chromatogr. B Analyt. Technol. Biomed. Life Sci. 1061–1062 (2017) 474–486, https://doi.org/10.1016/j.jchromb.20-17.07.021.
[25] K. Li, L.Q. Zhang, J. Nie, Study on UPLC-UV-MS fingerprints of different medicinal parts of *Poria cocos*, Zhong Yao Cai 36 (2013) 382–387, https://doi.org/10.13863/j.issn10014454.2-013.03.015.

[26] J.K. Mu, L. Zi, Y.Q. Li, L.P. Yu, Z.G. Cui, T.T. Shi, F. Zhang, W. Gu, J.J. Hao, J. Yu, X.X. Yang, Jiuzhuan Huangjing Pills relieve mitochondrial dysfunction and attenuate high-fat diet-induced metabolic dysfunction-associated fatty liver disease, Biomed. Pharmacother. 142 (2021) 112092, https://doi.org/10.1016/j.biopha.2021.112092.
[27] Y. Wei, R.S. Rector, J.P. Thyfault, J.A. Ibdah, Nonalcoholic fatty liver disease and mitochondrial dysfunction, World J. Gastroenterol. 14 (2008) 193–199.
[28] Q.L. Fang, X. Qiao, X.Q. Yin, Y.C. Zeng, C.H. Du, Y.M. Xue, X.J. Zhao, C.Y. Hu, F. Huang, Y.P. Lin, Flavonoids from Scutellaria amoena C. H. Wright alleviate mitochondrial dysfunction and regulate oxidative stress via Keap1/Nrf2/HO-1 axis in rats with high-fat diet-induced nonalcoholic steatohepatitis, Biomed. Pharmacother. 158 (2023) 114160.
[29] J.C. Arroyave-Ospina, Z. Wu, Y. Geng, H. Moshage, Role of oxidative stress in the pathogenesis of non-alcoholic fatty liver disease: implications for prevention and therapy, Antioxidants 10 (2021) 174, https://doi.org/10.3390/antiox10020174.
[30] R. Ramanathan, A.H. Ali, J.A. Ibdah, Mitochondrial dysfunction plays central role in nonalcoholic fatty liver disease, Int. J. Mol. Sci. 23 (2022) 7280, https://doi.org/10.3390/ij-ms23137280.
[31] X. Zhao, W. Qin, Y. Jiang, Z. Yang, B. Yuan, R. Dai, H. Shen, Y. Chen, J. Fu, H. Wang, ACADL plays a tumor-suppressor role by targeting Hippo/YAP signaling in hepatocellular carcinoma, npj Precis. Oncol. 4 (2020) 7, https://doi.org/10.1038/s41698-020-0111-4.
[32] M. Pawlak, P. Lefebvre, B. Staels, Molecular mechanism of PPARα action and its impact on lipid metabolism, inflammation and fibrosis in non-alcoholic fatty liver disease, J. Hepatol. 62 (2015) 720–733, https://doi.org/10.1016/j.jhep.2014.10.039.
[33] B. Liu, W. Yi, X. Mao, L. Yang, C. Rao, Enoyl coenzyme A hydratase 1 alleviates nonalcoholic steatohepatitis in mice by suppressing hepatic ferroptosis, American journal of physiology, Am. J. Physiol. Endocrinol. Metab. 320 (2021) E925–E937, https://doi.org/10.1152/ajpendo.0061-4.2020.
[34] Z. Xiao, Y. Chu, W. Qin, IGFBP5 modulates lipid metabolism and insulin sensitivity through activating AMPK pathway in non-alcoholic fatty liver disease, Life Sci. 256 (2020) 117997, https://doi.org/10.1016/j.lfs.2020.117997.
[35] H. Cortez-Pinto, H.Z. Lin, S. Yang, S. Odwin Da Costa, A.M. Diehl, Lipids up-regulate uncoupling protein 2 expression in rat hepatocytes, Gastroenterology 116 (1999) 1184–1193, https://doi.org/10.1016/s0016-5085(99)70022-3.
[36] K.D. Chavin, S. Yang, H.Z. Lin, J. Chatham, V.P. Chacko, J.B. Hoek, E. Walajtys-Rode, A. Rashid, C.H. Chen, C.C. Huang, T.C. Wu, M.D. Lane, A.M. Diehl, Obesity induces expression of uncoupling protein-2 in hepatocytes and promotes liver ATP depletion, J. Biol. Chem. 274 (1999) 5692–5700, https://doi.org/10.1074/jbc.274.9.5692.
[37] M. Sato, T. Tai, Y. Nunoura, Y. Yajima, S. Kawashima, K. Tanaka, Dehydrotrametenolic acid induces preadipocyte differentiation and sensitizes animal models of noninsulin-dependent diabetes mellitus to insulin, Biol. Pharm. Bull. 25 (2002) 81–86, https://doi.org/10.1248/bpb.2-5.81.
[38] H. Cai, Y. Cheng, Q. Zhu, D. Kong, X. Chen, I. Tamai, Y. Lu, Identification of triterpene acids in *Poria cocos* extract as bile acid uptake transporter inhibitors, Drug Metab. Dispos. 5 (2021) 353–360, https://doi.org/10.1124/dmd.120.000308.
[39] Y.H. Kuo, C.H. Lin, C.C. Shih, Dehydroeburicoic acid from antrodia camphorata prevents the diabetic and dyslipidemic state via modulation of glucose transporter 4, peroxisome proliferator-activated receptor α expression and AMP-activated protein kinase phosphorylation in high-fat-fed mice, Int. J. Mol. Sci. 17 (2016) 872.